UNIVERSITY OF INSUBRIA

Ph.D. SCHOOL OF EXPERIMENTAL AND TRANSLATIONAL MEDICINE

Department of Medicine and Surgery - Neuroscience division

XXXI cycle

Coordinator: Prof. Daniela Negrini

CDKL5 AND NEURONAL MORPHOLOGICAL DEFECTS: NOVEL PERSPECTIVES OF MICROTUBULE RELATED DRUGS

Ph.D. candidate: Diana Peroni

Tutor: Prof. Charlotte Kilstrup-Nielsen

Academic year 2017-2018

Table of contents

Summary

Mutations in the cyclin-dependent kinase like 5 (*CDKL5*) gene have been found in individuals with a rare neurodevelopmental disorder characterized by early-onset epileptic encephalopathy, severe intellectual disability, intractable seizures and infantile spasms (*1*, *2*). CDKL5 is a serine/threonine kinase with an N-terminal catalytic domain that shares homology with the mitogen-activated protein kinases and cyclin-dependent kinases. Its long C-terminal region of CDKL5 regulates several aspects of its properties such as the catalytic activity, subcellular localization and protein stability (*3*).

CDKL5 functions are still not fully understood: its localization in both the nucleus and the cytoplasm of expressing cells suggests that it may be involved in several cellular processes. In the nucleus CDKL5 interacts with MeCP2, DNA methyltransferase 1, the splicing factor SC35, and histone deacetylase 4 (HDAC4), thus suggesting a link between CDKL5 and gene expression (*4*–*7*). In neurons, cytoplasmic CDKL5 is distributed both in the soma and the neuronal periphery where its levels are tightly regulated in an activity-dependent manner. In the cytoplasm, CDKL5 is known to regulate several aspects of neuronal morphology through its interacting proteins. CDKL5 is involved in neuronal morphogenesis and dendritic arborization in a Rac1 dependent manner (*8*). Moreover, in accordance with its accumulation in the post-synaptic densities of mature neurons, CDKL5 was found to control proper spine development and synapse formation (*9*–*12*). A study in our laboratory has recently demonstrated a potential role of CDKL5 in axon specification and elongation (*13*), at least in part through its interaction with shootin1. The aberrant neuronal morphology linked to Cdkl5 has been observed both in *Cdkl5*-silenced primary neurons as well as in *Cdkl5*-null brains strongly suggesting that these defects may underlie the cognitive impairment characterizing both patients and mice devoid of the kinase. The molecular basis of these defects is still far from understood but altered cytoskeletal dynamics are likely to be involved.

The identification of IQGAP1 as novel CDKL5 interactor may provide a key to understand such neuronal defects [Appendix 1, (*14*)]. IQGAP1 promotes microtubule (MT) dynamics through its association with Rac1 and the MT plus-end binding protein (+TIP) CLIP-170 (*15*). In cycling cells, CDKL5 controls the localization of IQGAP1 at the cell cortex and the

formation of the Rac1–CLIP-170–IQGAP1 complex, thus allowing the guidance and capture of MTs at the cell cortex. In particular, CLIP-170 activity on MTs might play a significant role in the regulation of cytoskeletal dynamics in cycling cells and neurons. Considering how the loss of CDKL5 negatively impacts on cellular and neuronal morphology, we envisaged that this kinase could regulate cytoskeletal dynamics acting directly or indirectly on CLIP-170. Indeed, CLIP-170 is known to regulate several aspects of neuronal morphology such as axon outgrowth (*16*), dendritic arborization (*17*) and growth cone organization. By bridging the actin cytoskeleton to MTs, CLIP-170 coordinates proper cytoskeletal dynamics (*18*). The binding of CLIP-170 to MTs and its partners is tightly regulated by its conformational state; it has been demonstrated that the intramolecular association between the N- and C-termini results in autoinhibition of CLIP-170, thus altering its binding to MTs (*19*).

In the current study, we analysed the role of CDKL5 in the regulation of CLIP-170 activity. Through a FRET analysis on COS7 cells we demonstrated that the loss of CDKL5 causes CLIP-170 to be mainly in its closed inactive conformation, thus reducing its interaction with MTs.

Furthermore, using *Cdkl5*-KO primary hippocampal neurons we demonstrated that the loss of CDKL5 is detrimental for the correct progression of the early steps of neuronal differentiation. In fact, the absence of CDKL5 influenced the distribution of MTs at the axonal growth cone level. Altered MT dynamics in the growth cones correlated with disrupted axon polarization and decreased axonal elongation. Moreover, our characterization of *Cdkl5*-KO neurons confirmed the role of this kinase in the formation and maturation of dendritic spines.

As previously mentioned, CLIP-170, acting on MT dynamics, is known to regulate multiple aspects of neuronal morphology, such as proper growth cone organization and size, axon specification and elongation (*16*) and dendritic arborization (*17*). Moreover, even if a direct link has not been demonstrated yet, CLIP-170 may play a role in the regulation of spine formation and maturation, as +TIPs are known to coordinate MT dynamics in such compartment (*20*).

Considering all above we investigated the localization of CLIP-170 in axonal growth cones and in dendritic spines in *Cdkl5*-KO neurons. We found that this +TIP is present in both cellular compartments. Intriguingly, we found that the loss of Cdkl5 causes its

delocalization from tubulin at the growth cone level and alters its entrance in dendritic spines. These results strengthen the hypothesis that CDKL5 and CLIP-170, acting in common pathways, may regulate cytoskeletal dynamics in such compartments.

We recently demonstrated that the neurosteroid Pregnenolone (P5) is able to revert several altered morphological phenotypes both in CDKL5 depleted proliferating cells and in *Cdkl5*-silenced neurons [Appendix 1, (*14*)]. By binding CLIP-170 this compound stabilizes the extended conformation of the protein, thus increasing its affinity for MTs and promoting MT polymerization (*21*). Hence, we hypothesised that P5 might be sufficient to bypass the need of CDKL5, restoring the morphological defects associated with the loss of the kinase.

In the current study we showed that morphological and molecular defects found in *Cdkl5*-null neurons and the altered dynamics of CLIP-170 on MTs in COS7 cells can be restored upon treatment with P5. Moreover, we evaluated the efficacy of the synthetic non-metabolizable derivative, Pregnenolone-Methyl-Ether (PME). This compound raised our interest as it may represent an interesting alternative to P5 in a future clinical application. Indeed, while maintaining the same biological action, PME is devoid of the undesired side effects due to the metabolism of P5 (*22*). Intriguingly, the positive effects obtained in neurons with the treatment with P5 could also be achieved with PME. Furthermore, both compounds increased the activity of CLIP-170, promoting its open extended conformation and its affinity for MTs in COS7 cells. Considering all above, we speculate that the positive effects of the two compounds are likely to be due to an activation of CLIP-170 functionality and a concomitant increase in MT dynamics.

Altogether, our findings are conceivably shedding light on the molecular mechanisms through which Cdkl5 exerts its role in neuronal development and maturation, accelerating the design of novel therapeutic strategies for CDKL5 disorder.

1. Introduction

1.1 From Rett Syndrome to CDKL5 disorder

Rett syndrome (RTT; OMIM 312750) is an X-linked dominant neurodevelopmental disorder occurring almost exclusively in females (*23*) and considered the second genetic cause of female intellectual disability after Down Syndrome (*24*) as it affects approximately 1 in 10000 female birth. RTT is characterized by a wide spectrum of clinical manifestations: in the classic form, after a period of normal development (the first 6-18 months of life), patients show a developmental stagnation followed by a regression phase in which they loose acquired abilities such as hand use, learned single words and communicative behaviour (*25*). Typical additional RTT manifestations are growth retardation, motor dysfunction, postural hypotonia, along with stereotyped hand movements and autistic like symptoms (such as lack of social smiling, hypersensitivity to sound, lack of eye-to-eye contact) (*26*). In the last phase of the disease, cardiac abnormalities, respiratory problems, epileptic seizures and Parkinsonian features arise (*27*). Approximately 95% of patients with classic RTT show a mutation in the methyl CpG-binding protein 2 gene (*MECP2*; OMIM 300005 (*28*), which usually arises *de novo*. However, beside classical RTT, atypical forms, with milder or more severe clinical pictures, have been described and clustered into three distinct clinical groups: the preserved speech variant, the early seizure variant (ESV), and the congenital variant (*29*). Among these atypical forms, mutations in *MECP2* appear only in 50-70% of cases (*30*), suggesting the existence of other genes involved in RTT. In 1985 Hanefeld described for the first time the ESV RTT variant, also known as the Hanefeld variant, in a female patient presenting infantile spasms followed by several symptoms consistent with the diagnosis of RTT (*31*). No *MECP2* mutations have been reported in patients with this variant, suggesting that most cases of RTT with early onset seizures are caused by a different mechanism (*32*). The *CDKL5* (*cyclin-dependent kinase-like 5*) gene, also known as STK9 (Serine Threonine Kinase 9), was firstly identified through a transcriptional mapping effort of disease genes of the human Xp22 region, already known to be associated with different pathologies, including Nance-Horan (NH)

syndrome, oral-facial-digital syndrome type 1 (OFD1), and a novel locus for non-syndromic sensorineural deafness (DFN6) (*3*). The first correlation between mutations in *CDKL5* and neuronal diseases was suggested in year 2000, when genetic deletions in two Danish siblings affected by retinoschisis (RS) and epilepsy were analysed. In this study, a large deletion of 136 kb was found to partly delete *RS1* (X-linked juvenile retinoschisis precursor protein) and *PPEF1* (protein phosphatase gene with EF calcium-binding domain), and truncate the 3' end of the *CDKL5* gene. Since mutations in *RS1* and *PPEF1* had never been associated with seizures, the most plausible hypothesis was that epilepsy in these patients was caused by deletions of the C-terminal region of CDKL5 (*33*). Later on, in 2003, the link between *CDKL5* mutations and neurological diseases was further strengthened by the description of two different truncations of the gene in two girls suffering from West syndrome, an infantile syndrome characterized by infantile spasms, hypsarrhythmia, and severe-to-profound mental retardation (*1*). The first strong indications of a direct involvement of *CDKL5* in the Hanefeld variant of RTT came in 2004, when *de novo* mutations in the catalytic domain of CDKL5 were identified in patients with early-onset infantile spasms and clinical features overlapping those of RTT (*34*). Moreover, frameshift *CDKL5* mutations were identified in patients from two unrelated families with severe early-onset epilepsy with infantile spasms, mental retardation and clinical manifestations similar to RTT (*34*, *35*). Lastly, Scala and colleagues described *CDKL5* frameshift deletions in patients with the ESV variant characterized by the development, in the very first post-natal weeks of life, of drug resistant convulsions, usually of the spasm type. They also analysed *CDKL5* in *MECP2* negative patients with classical RTT or the preserved speech variant, but no mutations were found (*36*). Since then, numerous articles highlighted the correlation between *CDKL5* mutations and clinical pictures characterized by early-onset epilepsy, myoclonic encephalopathy, intractable neonatal seizures, severe infantile encephalopathy, mental retardation, and autistic features with intellectual disability. In order to simplify the terminology, these phenotypes have been gathered together under the name of "*CDKL5*-related disorder" or "*CDKL5*-associated encephalopathy" (*37*).

Considering all the above, CDKL5 disorder (CD) is currently considered as an independent clinical entity associated with early-onset encephalopathy (*2*), separate to RTT, rather than another variant.

1.2 CDKL5 disorder: defining the clinical features

A full clinical picture of CD is still limited as a broader number of patients is needed to delineate more thoroughly the natural history of this disease and to identify its main characteristics to better define the diagnostic criteria. The first characterization of CD patients came in 2008 when Bahi-Buisson and colleagues screened the whole coding region of *CDKL5* in a total of 183 female patients with early seizure encephalopathy and described the clinical features of 20 patients with pathogenic CDKL5 mutations. They found that the main phenotypic manifestations differed depending on age: in younger patients (≤2 years of age), epileptic seizures, starting within the first 3 months of life, hypotonia, and poor eye contact represented the main sign of CDKL5 mutations. Conversely, from the age of 2-3 years, severe encephalopathy associated with epilepsy and RTT-like features (apraxia, stereotypic movements, sleep disorders) were predominant (*37*). Moreover, they stressed that early epilepsy (median age of onset 4 weeks) is a key to identify the patients likely to have CDKL5 mutations. Concerning this, the authors described a three-step pattern of epilepsy: stage I (onset 1-10 weeks) of "early epilepsy" consists of frequent convulsive seizures characterized by high frequency (2-5 per day); during stage II (from 6 months to 3 years of age) seizures decrease but patients develop epileptic encephalopathy with infantile spasms and hypsarrhythmia. Eventually, in stage III, half of patients recovered, with fewer seizure number, while the other half developed refractory epilepsy with tonic seizures and myoclonia (*38*). More recently, the increased number of patients affected by CD allowed a further investigation of clinical diagnostic criteria of the CD. Artuso and colleagues tried to delineate the specific clinical diagnostic criteria for CD reporting an investigation of 9 girls with CDKL5 mutations compared with 34 cases already reported in literature (Fig 1.1). According with previous studies, the authors confirmed that all CDKL5 patients experienced seizures during their lives: early onset epilepsy was thus defined as the main criteria for the identification of CDKL5 mutations. The presence of stereotypic hand movements was also indicated as a hallmark of the disease, in addition to normal prenatal history and a quite normal perinatal period, severe hypotonia, poor eye contact and the absence of response to social interactions, absence of speech, and hand skills and the presence of gastrointestinal disturbances and breathing irregularities

(*39*). These criteria started to lay the foundations for a specific characterization of CD, distinguishing it from the other forms of RTT.

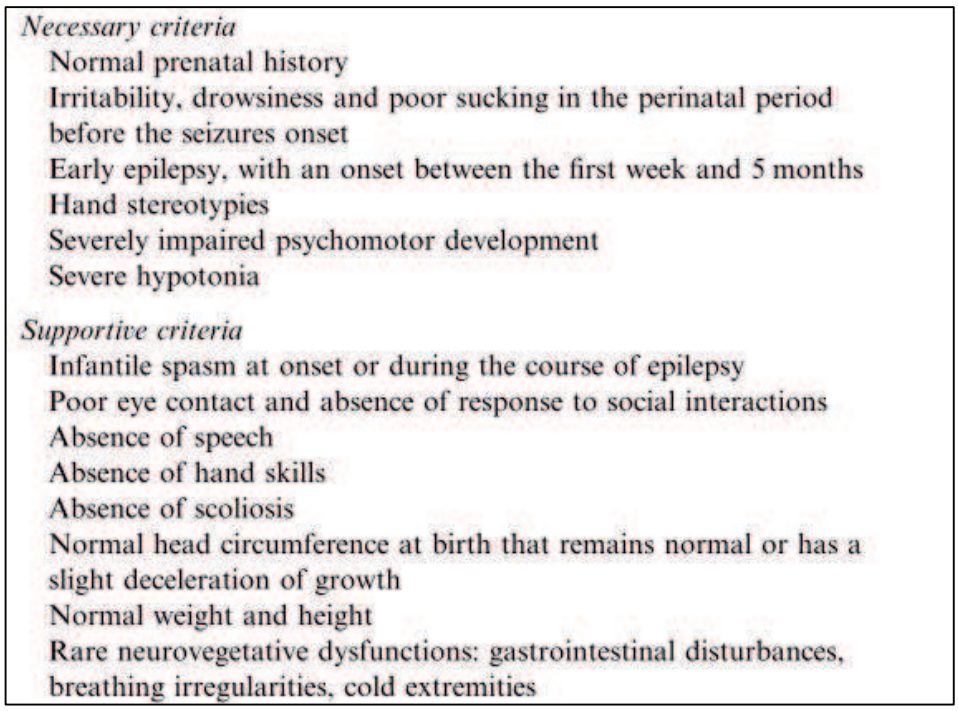
Necessary criteria
Normal prenatal history
Irritability, drowsiness and poor sucking in the perinatal period before the seizures onset
Early epilepsy, with an onset between the first week and 5 months
Hand stereotypies
Severely impaired psychomotor development
Severe hypotonia

Supportive criteria
Infantile spasm at onset or during the course of epilepsy
Poor eye contact and absence of response to social interactions
Absence of speech
Absence of hand skills
Absence of scoliosis
Normal head circumference at birth that remains normal or has a slight deceleration of growth
Normal weight and height
Rare neurovegetative dysfunctions: gastrointestinal disturbances, breathing irregularities, cold extremities

Fig. 1.1 Diagnostic criteria for early-onset seizure variant of RTT (*39*)

The expanded knowledge about RTT and related disorders, along with the increased number of patients mutated in *CDKL5* pushed to outline specific diagnostic criteria for these diseases. In 2010, Neul and colleagues, in collaboration with the RettSearch Consortium, revised and simplified the diagnostic criteria for typical and atypical RTT (Fig. 1.2). Three groups of criteria were identified: four *main* criteria required for both typical and atypical RTT, *exclusion* criteria for typical RTT and *supportive* criteria for atypical RTT. The diagnosis of atypical RTT, requires that, beside the presence of regression, at least 2 out of 4 main criteria and 5 out of 11 specific supportive criteria should be present. In addition, some clinical features were specified to distinguish the three variant forms, among which the ESV. Notably the presence of a period of regression followed by recovery was considered as required criterion for both typical and atypical RTT (*40*).

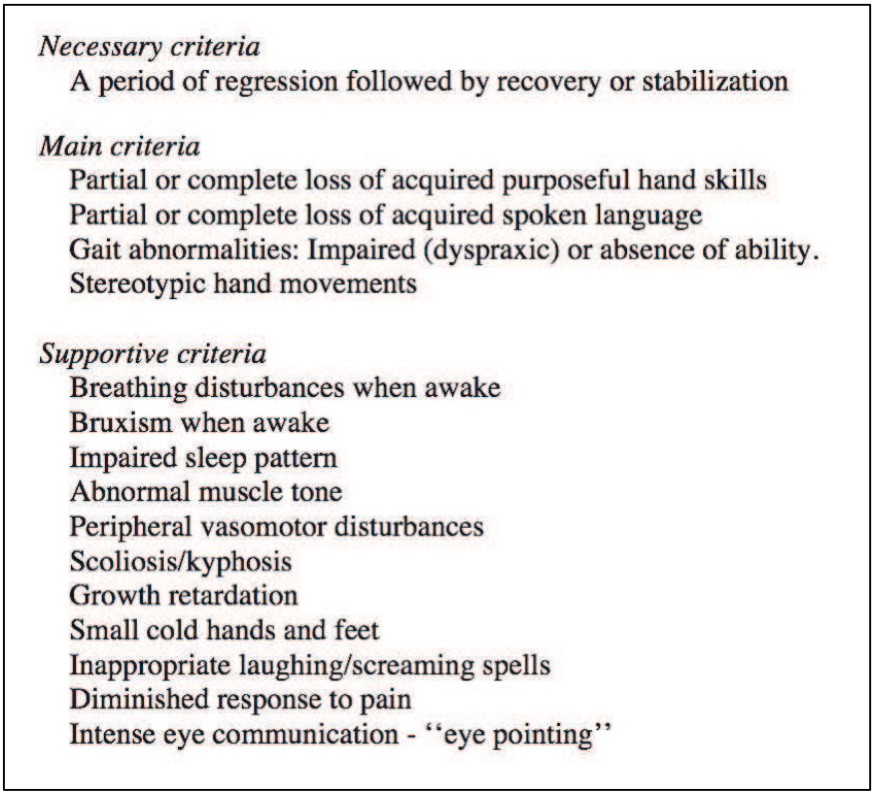

Fig. 1.2 Diagnostic criteria for typical and atypical Rett (*40*)

In 2013, CDKL5 disorder was suggested to be an independent clinical entity that should not be considered as part of the RTT spectrum (*2*). Indeed, among 77 females (6 months to 22,4 years of age) and 9 males (1.1 to 14.9 years of age) with a pathogenic or potentially pathogenic *CDKL5* mutations, 25% of females and no males fulfilled the previously described criteria for ESV RTT. These unexpected results were largely due to the absence of a period of regression in the majority of cases, in accordance with previous studies (*37*, *39*). Also specific supportive criteria, such as diminished response to pain, spinal curvature and intensive eye pointing, were infrequently reported (Fig. 1.3).

Extremely likely

Seizures within the first year of life (90% by 3 months)
Global developmental delay Severely impaired gross motor function

Very likely

Sleep disturbances
Abnormal muscle tone
Bruxism
Gastrointestinal issues

Likely

Subtle dysmorphic features including three or more of the following: broad/prominent forehead; large 'deep-set' eyes; full lips; tapered fingers; and anteverted nares in males
Hand stereotypies
Laughing and screaming spells
Cold hands or feet
Breathing disturbances
Peripheral vasomotor disturbances

Unlikely

Independent walking
Microcephaly
Major congenital malformations

Fig. 1.3 Clinical features suggesting a diagnosis of the CDKL5 disorder (*2*)

Interestingly, some dysmorphic features were identified as useful for the diagnosis of CD (Fig. 1.4). Indeed, CD patients are frequently characterized by prominent and/or broad forehead, high hairline, relative midface hypoplasia, deep-set but large appearing eyes and infra-orbital shadowing (*2*).

Fig. 1.4 Examples of facial, hand and feet features in females (a-g) and males (h) with the CDKL5 disorder (*2*).

Even if it seems that CDKL5 mutated boys are more severely affected than females, it is still difficult to make a comparison between sexes. Random X-inactivation, which in females produces a mosaic expression of normal and altered CDKL5, may result in a less severe outcome. A huge heterogeneity exists between patients suggesting that the phenotypic differences could be due to modifier genes that have been differentially influenced by environmental and/or epigenetic factors. Further studies focused on the identification of direct and indirect partners of CDKL5, will help defining its functions and might lead to the identification of modifier genes representing relevant targets for therapeutic approaches (*41*).

1.3 The *CDKL5* gene

The human *CDKL5* gene occupies approximately 240 Kb of the Xp22.13 chromosomal region and it is composed of 27 exons. The first three (exons 1, 1a, 1b) are untranslated and the ATG start codon is located within exon 2, implying that the coding sequences are contained within exons 2-21 (*1*, *42*). *CDKL5* is known to undergo alternative splicing, which result in the formation of at least 5 different isoforms (hCDKL5-1-5, Fig. 1.5). The first isoforms were discovered in 2003 by Kalscheuer and colleagues, but a detailed *CDKL5* mRNA analysis led to a more complete picture in 2016. hCDKL5-1 (107 KDa; 960 amino acids) is the prevailing isoform in the central nervous system of both human and mouse (mCdkl5-1), validating this animal as a model for studying the neurological functions of CDKL5. Exon 17, whose the function is still unknown, is present in hCDKL5-2-4 (mCdkl5-2) isoforms that differ only slightly from hCDKL5-1, but have a lower expression in brain. hCDKL5-5 (previously $CDKL5_{115}$, 115 KDa, 1030 amino acids) is the only isoform presenting exons 20-22 and is mainly expressed in testes (*43*).

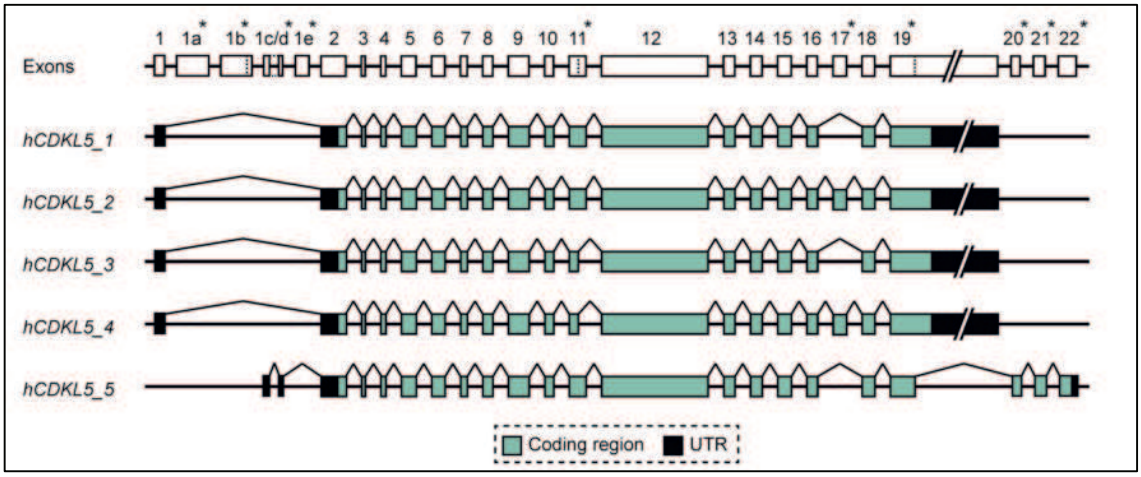

Figure 1.5 Schematic representation of the structure of the human *CDKL5* gene and the composition of the different coding isoforms (hCDKL5-1-5). Splice events are indicated by lines between exons. Differences among the isoforms are indicated by asterisks. Alternative splice sites are indicated by dotted lines within exons (*43*).

The murine isoforms mCdkl5-1-2 are orthologous of their human counterparts. In contrast, the coding regions of the other three mouse transcripts do not show full orthology to human isoforms and are hence termed mCdkl5-6, mCdkl5-7 and mCdkl5-8 (Fig. 1.6)

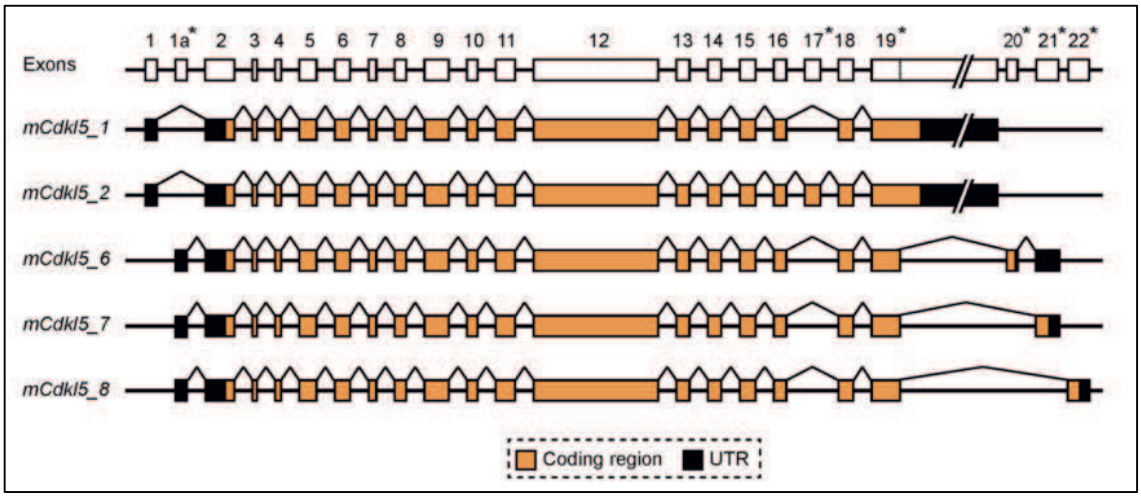

Figure 1.6 Schematic representation of the structure of the mouse *Cdkl5* gene and the composition of the different coding isoforms (mCdkl5-1,2,6-8). Splice events are indicated by lines between exons. Differences among the isoforms are indicated by asterisks. Alternative splice sites are indicated by dotted lines within exons (*43*).

1.4 The CDKL5 protein

CDKL5 belongs to the CMGC family of serine/threonine kinases, which includes cyclin-

dependent kinases (CDKs), mitogen-activated protein kinases (MAPKs), glycogen synthase kinases (GSKs) and CDK-like kinases (*3*). Indeed, CDKL5 is characterized by a highly conserved NH_2-terminal catalytic domain (amino acids 13-297), homologous to that of the other CDKL-family members and a long (600 amino acids) COOH-terminal tail. This region, which is unique for CDKL5 and distinguishes it from other proteins, is highly conserved between different CDKL5 orthologs that differ only in the most extreme C-terminus, suggesting a potential crucial role. The catalytic domain comprises an ATP-binding region (amino acids 19-43), a serine-threonine kinase active site (amino acids 131-143), and a conserved TEY (Thr-Xaa-Tyr) motif within its activation loop (amino acids 169-171) (*44*) whose dual phosphorylation is required for activation of extracellular signal-regulated kinases (ERKs) (*45*); in addition, CDKL5 contains an autocatalytic activity directed against its TEY motif. The long C-terminal domain contains two distinct putative signals for nuclear import (NLS1 and NLS2; amino acids 312-315 and 784-789 respectively) and export (NES, amino acids 836-845): accordingly the COOH-terminal region plays an important role in localizing the kinase properly within the nuclear compartment (Fig. 1.7) (*44*). The precise consensus sequence within CDKL5 substrates has not yet been fully characterized. The CDKL5 interactor Amph1 and its homologue (not phosphorylated by CDKL5) have been used in a recent study in which RPXSX emerged as a putative consensus sequence (*46*). However, this sequence is not present in other CDKL5 substrates, suggesting that further investigations are needed to better understand the molecular basis that regulate the relationship between CDKL5 and its interactors.

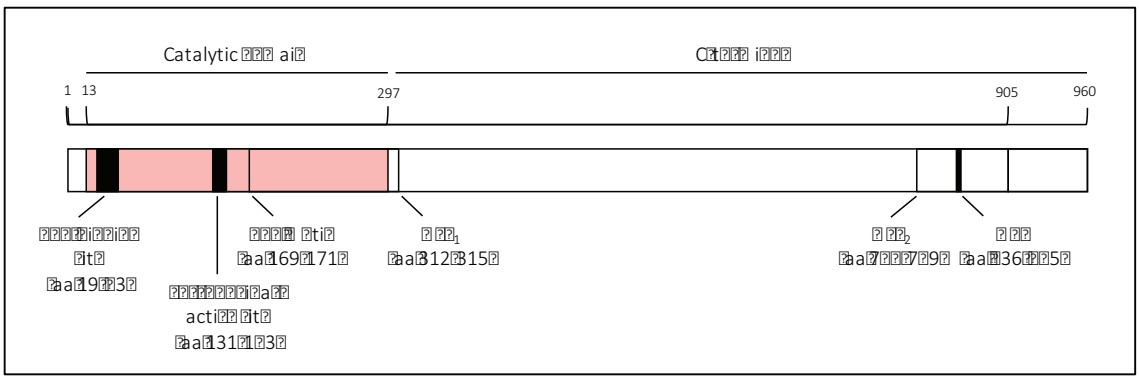

Fig. 1.7 Schematic representation of human CDKL5 protein with the functional domain and signature indicated. NLS: nuclear localization signal. NES: nuclear export signal. Kinase domain is depicted in pink [adapted by (*41*)]

1.5 CDKL5 pathological mutations

CDKL5 pathogenic mutations, which generally occur *de novo*, are distributed throughout the entire sequence and include missense and non-sense mutations, splice variants (*47*), exonic deletions/duplications, in-frame and frameshift deletions or insertions, and multiple mutations. Missense mutations involve almost exclusively the catalytic domain, while they are unlikely to be pathogenic when occurring elsewhere in the protein (*48*). Truncating mutations can occur anywhere in the gene, resulting in CDKL5 derivatives of various lengths (Fig. 1.8).

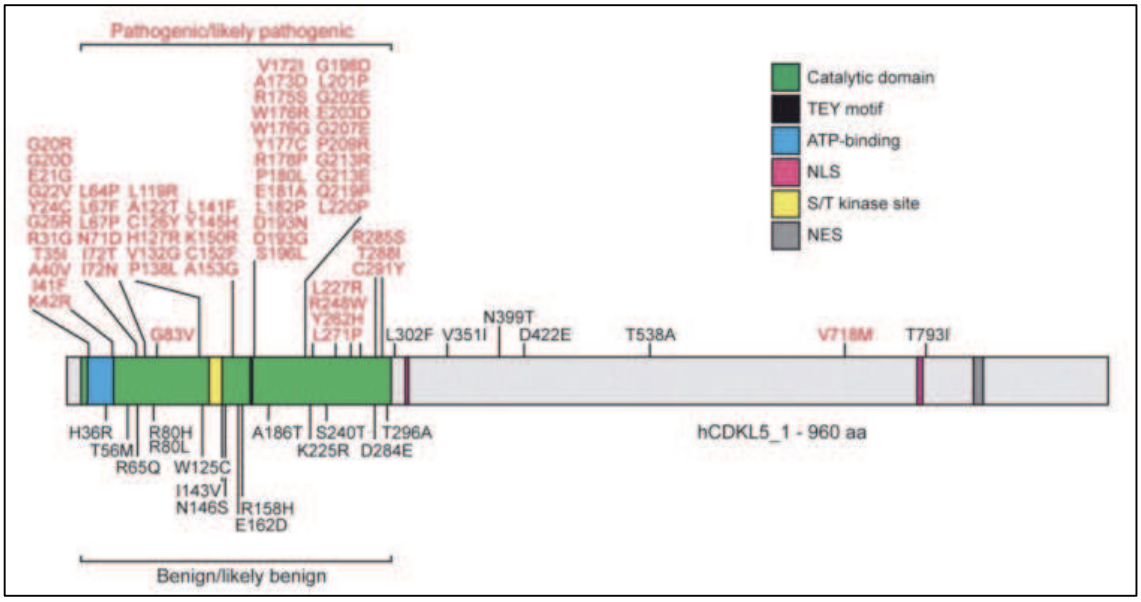

Figure 1.8 Pathogenic CDKL5 missense variants in patients [adapted by (*48*)]

The overexpression of mutated CDKL5 derivatives in non-neuronal cell lines has allowed elucidating the molecular effects of some pathological mutations. Some missense mutations in the kinase domain cause a great reduction of the catalytic activity of CDKL5 while C-terminal truncating mutations produce an increased catalytic activity and the nuclear accumulation of the kinase (*44*, *49*). These results suggest the importance of the C-terminal tail in controlling the activity (acting as negative regulator) and the subcellular localization of CDKL5. However, it is important to take into account that several truncating mutations generate transcripts which are likely to be highly unstable, due to mRNA surveillance and nonsense-mediated mRNA decay (NMD) phenomenon (*37*). Several other studies proposed that mutations in the catalytic domain are

associated with a more severe clinical phonotype, characterized by a higher incidence and more precocious onset of epileptic encephalopathy than that caused by truncating mutations (*38*, *50*). Furthermore, recent studies have highlighted the importance of CDKL5 dosage. Indeed, Szafranski and colleagues reported of 11 patients with genomic duplications involving *CDKL5* characterized by neurodevelopmental and neurobehavioral characteristics including difficulties in learning, autistic and hyperactive behaviour, developmental and speech delay. Interestingly, none of these patients presented epilepsy. Thus, increased dosage of CDKL5 seems to affect the global output of the interactions with its substrates, leading to perturbation of synaptic plasticity and development (*51*).

So far, no clear genotype-phenotype correlation of *CDKL5* mutations has been established. Such prediction is still difficult due to the limited number of patients and the small number of recurrent mutations. In addition, the clinical phenotypes among patients with recurrent mutations are heterogeneous. This is likely due to the X-linked status of *CDKL5* and that the majority of patients are heterozygous females. As a result of random X-chromosome inactivation (XCI), female patients carrying the same genetic mutation can have different mosaic expression of *CDKL5*, thus resulting in a spectrum of phenotypes (*52*). Males carrying *CDKL5* mutations in general show a more severe epileptic encephalopathy than girls (*53*) in line with the expression of mutated CDKL5 in all cells.

The phenotypes associated with *CDKL5* mutations encompass milder forms, with controlled epilepsy and ability to walk, to a severe form with absolute microcephaly, virtually no motor development, and refractory epilepsy (*37*). As at July 2018, 255 *CDKL5* variants were listed in the RettBASE (RettSyndrome.org Variation Database – mecp2.chw.edu.au), comprising 64,3% of pathogenic or likely pathogenic mutations, benign or likely benign mutations and variants of unknown significance (VOUS, Fig. 1.9).

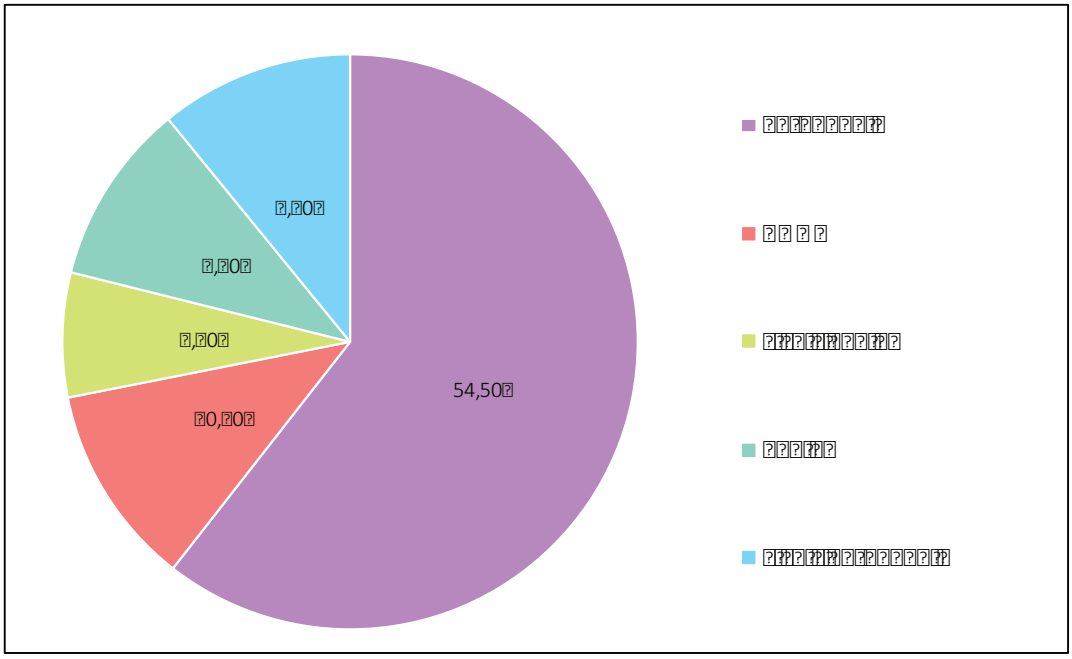

Fig. 1.9 Schematic illustration of the pathogenicity distribution among CDKL5 variants (adapted by RettBASE).

1.6 CDKL5 expression and subcellular localization

Since the identification of *CDKL5* and its involvement in neurological diseases, expression studies in human and mouse tissues have shown that *CDKL5*/*Cdkl5* mRNA is present in the brain, where the transcripts levels are the highest, and in a wide range of other tissues such as lung, spleen, testis, prostate, uterus, placenta and thyroid (*3*, *42*, *43*). A detailed analysis of *Cdkl5* expression in the adult mouse brain showed that transcript levels are particularly abundant in the most superficial cortical layers of the adult forebrain. The high expression levels in the frontal cortical areas, such as motor, cingulate and pyriform cortex, suggest a function of Cdkl5 in the physiology of these brain districts, responsible for higher order functions like language and information processing. Moreover, the hippocampus, a brain area that regulates learning and memory, shows a large amount of *Cdkl5* mRNA in all the *Co*[illegible] fields. Interestingly, very high levels of *Cdkl5* transcripts are detected in several thalamic nuclei, involved in sensory and motor signal relay and in the regulation of consciousness and sleep, whereas lower levels are detected in the cerebellum. Considering the fair expression of the kinase transcripts in the striatum, glutamatergic and GABAergic neurons appear to be the two cell types expressing most of the brain *Cdkl5*. Conversely,

dopaminergic areas (such as the *substantia nigra* or the ventral tegmental area) and noradrenergic areas (such as the *locus coeruleus*) express very low levels of *Cdkl5* (*41*). In addition to the neuronal expression, *Cdkl5* has also been detected at low level in the glia. Western blot analyses of Cdkl5 protein expression pattern in mice and rats more or less confirmed the transcript profile in adult brain (*8*, *49*). Cdkl5 protein levels reach the highest in conjunction with the development and differentiation of the brain. Indeed, Cdkl5 is only weakly present during embryogenesis, but gets strongly induced during the postnatal stages until P14, where after it slowly declines (*49*). As mentioned, isoform 1 is the most abundant during the period of neuronal development in both human and mouse, strengthening the hypothesis of its central role in the process of neuronal maturation. Conversely, in adult brain all isoforms are expressed at higher levels than in the foetal one, whereas hCdkl5 5 is present only in the foetal brain (*43*). The functional significance of different *Cdkl5* transcript isoforms expression profiles and levels during pre- and post-natal development still remains to be assessed.

At the subcellular level, CDKL5 has been found to shuttle between the cytoplasm and the nucleus. In the latter compartment it seems to regulate alternative splicing events and gene expression through its interaction with SC35 (*6*), MeCP2 (*4*) and DNMT1 (*5*). It is noteworthy that CDKL5 seems to be excluded from the cell nucleus during embryogenesis and becomes nuclear only during early postnatal stages, concomitantly with the strong induction of expression correlating with neuronal maturation (*49*). □

1.7 Multiple roles of CDKL5

□

Although there have been important steps towards an increased knowledge of CDKL5 functions since the discovery of its involvement in neurological disorders, more are still needed to allow the development of therapeutic strategies for CD.

Several studies have demonstrated the potential role of CDKL5 in the neurodevelopment and in the maintenance of proper neuronal activity. Since CDKL5 is a protein kinase, the analysis of how phosphorylation profiles are altered by its absence represents a good starting point to define the possible molecular pathways regulated by CDKL5.

A serine/threonine kinome study revealed that many signal transduction pathways are disrupted in *Cdkl5*-knock out (*Cdkl5*-KO) brains. Among them, the AKT-mTOR pathway appeared to be more strongly affected. Indeed, the absence of Cdkl5 produced reduced phosphorylation of mTOR, a well known regulator of cell growth, proliferation, motility and neuronal plasticity (*54*), and AKT, with a consequent decreased phosphorylation of its substrates such as the ribosomal protein S6 (rpS6), a modulator of protein translation (*55*, *56*). Interestingly, the deregulation of such pathway has already been linked to autism spectrum disorders (ASDs), RTT and epileptic encephalopathies, suggesting that this may be a common signalling deficit in these pathologies (*57*, *58*). Moreover, loss of Cdkl5 was demonstrated to alter the phosphorylation profiles of kinases involved in synaptic plasticity, including PKA and PKC, as well as kinases involved in cellular metabolism. Although many of these alterations may be indirect effects of the loss of CDKL5, they point out the role of this kinase in the coordination of multiple signalling pathways (*55*).

Consistently, the homology between CDKL5 and members of the MAPKs and CDKs, well known regulators of cell cycle progression, has pushed forward the study of its possible role also in proliferating cells. In this regard, in 2014 Fuchs and colleagues illustrated that Cdkl5 is involved in regulating the process of adult neurogenesis: indeed, an increased proliferating rate of neuronal precursor cells (NPC) was observed in the hippocampus of adult *Cdkl5*-KO mice, in comparison with the wild type (WT) counterpart, suggesting negative role of the kinase in cell proliferation. On the other hand, they highlighted an increase in apoptotic cell death of post-mitotic granule neuron precursors, with a reduction in total number of granule cells, indicating a decreased survival rate of new-born cells in *Cdkl5*-KO mice. No difference was found in the number of astrocytes, demonstrating that loss of Cdkl5 specifically affects the survival of post-mitotic neurons without influencing astrogliogenesis (*59*). Moreover, these defects were associated with an impairment of AKT/GSK3 signalling pathway, regulating diverse developmental events in the brain, including neurogenesis, neuron survival and differentiation. Indeed, loss of Cdkl5 leads to a decreased phosphorylation of GSK3, leading to its activation. Considering that GSK3 is known to exert a crucial inhibitory regulation of neurite outgrowth, synapse formation, neurogenesis and

survival of newly-generated neurons (*60*), these data suggested that the loss of Cdkl5 may impair neuron survival and maturation by disrupting the AKT/GSK3β signalling pathway (*59*).

These data suggested an implication of CDKL5 in the regulation of cell cycle progression, a role which has recently been further confirmed in our laboratory: indeed, CDKL5 was found to contribute to faithful cell division, mediating the correct formation of mitotic spindle formation and regulating cytokinesis (*61*). An implication of CDKL5 in the control of cell cycle progression could explain the defects in neuronal progenitor proliferation and survival, which are altered in *Cdkl5*-KO mice (*59*). Interestingly, several studies have highlighted that such deficits in the regulation of cell proliferation and differentiation in neural stem cells are a convergence point across many neurodevelopmental disorders (*62*).

Taking a step backwards, the first CDKL5 interactor was identified in 2005 by Mari and colleagues. In their study the authors characterized two patients carrying mutations in *CDKL5* and diagnosed with the ESV of RTT. Given that *MECP2* and *CDKL5* mutations cause a similar phenotype, they investigated whether the two proteins belong to the same molecular pathway. The identification of a spatial and temporal overlapping expression of the two genes led to the hypothesis that the two proteins could act in the same developmental pathway. In contrast, different expression levels indicated that in some circumstances, the two genes are regulated independently. Moreover, they demonstrated that the two proteins interact *in vitro* and *in vivo* and that CDKL5 mediates MeCP2 phosphorylation *in vitro*. Even though it is still unclear whether this happens also *in vivo*, it is known that specific events of MeCP2 phosphorylation are required to regulate, among other functions, gene transcription during learning and memory, proper dendritic/synaptic development and behavioural responses to experience (*63*, *64*), and cell proliferation, division, migration and differentiation. This suggests that, even though CD and RTT are two distinct clinical entities, they may share common molecular pathways, which could explain, at least in part, the common features between the two pathologies (*4*, *65*).

As mentioned, CDKL5 has been found to co-localize and interact directly with MeCP2, a dynamic epigenetic factor that is a well-known interactor of DNMT1 (DNA methyltransferase 1), an enzyme that controls the maintenance of genomic DNA methylation. Kameshita and colleagues demonstrated that CDKL5 can bind to the N-terminal domain of DNMT1 and may therefore play a role in epigenetics and gene expression (*5*).

With regard to the localization of CDKL5 within the nuclear compartment, the kinase localizes and is associated with the splicing factor SC35 clustered in the so-called nuclear speckles. This evidence has suggested yet another role of CDKL5 in the regulation of the nuclear trafficking of splicing machinery (*6*).

Lastly, HDAC4 (histone deaceltylase 4) has been identified as a direct phosphorylation target of CDKL5. HDAC4 is highly abundant in neurons, where it is mainly located in the cytoplasmic compartment thanks to its specific phosphorylation. Cdkl5-mediated phosphorylation controls the cytoplasmic retention of HDAC4; consistently, loss of Cdkl5, increases the nuclear translocation of HDAC4 nuclear translocation is accompanied by a decrease in histone acetylation and may, in turn, produce a number of cellular effects through epigenetic and non-epigenetic mechanisms of gene regulation, which may contribute to the brain phenotype of CDKL5 disorder (*7*).

On top of this, the regulation of cell morphology has emerged as a central role of CDKL5. In the last years, after the generation of *Cdkl5*-KO mouse models, several studies have demonstrated that the loss of Cdkl5 negatively impacts on the proper morphological development of neurons (Fig. 1.10). Indeed, *Cdkl5*-KO cortical and hippocampal pyramidal neurons showed reduction of dendritic arborization with a significant decrease in cortical thickness (*56*, *59*). These data confirmed previous evidences obtained with RNA interference in cultured rat cortical neurons, which were also characterized by a reduction of total length of both dendrites and axons (*8*). This aspect was confirmed by Ricciardi an colleagues, who investigated the role of Cdkl5 in dendritic spines: the co-localization of Cdkl5 with post-synaptic density protein 95 (PSD95) and netrin-G1 ligand (NGL-1), and its juxtaposition to the vesicular glutamate transporter (VGLUT), led the authors to relate Cdkl5 to glutamatergic synapses (*9*, *10*). Cdkl5 synaptic targeting is promoted by its interaction with the palmitoylated form of

PSD95 or by the formation of a complex involving PSD95 and NGL-1, a synaptic cell adhesion molecule that exerts a regulatory role in synapse formation and homeostasis; its phosphorylation at Serine 631, mediated by Cdkl5, is necessary to ensure stable binding to PSD95. The synaptic presence of Cdkl5 suggests its involvement in molecular pathways that regulate synaptic maturation and function. Indeed, hippocampal neurons silenced for *Cdkl5* showed an increased percentage of filopodia-like and thin-headed spines, characteristic of an immature stadium of spine development. Moreover, the morphological alterations reported in *Cdkl5*-silenced neurons were associated with a reduction in the number of excitatory synapses and synaptophysin *puncta* *in vitro* and *in vivo*, as well as in induced pluripotent stem cell (iPSC) lines from two females diagnosed with *CDKL5* pathological mutations (*9*). Similar results were obtained in *Cdkl5*-null brains, which showed a decrease in excitatory synaptic *puncta* in the *Cornu* *Ammonis* field of hippocampus as result of a lower spine density. Furthermore, immunohistochemical characterization of spine shape revealed a higher percentage of immature spines (filopodia, thin- and stubby-shaped) in *Cdkl5*-KO neurons compared to wild type neurons (WT) (*7*). Recently, Della Sala and collaborators, through an *in vivo* two-photon microscopy of the somatosensory cortex of *Cdkl5*-KO mice, monitored structural dynamics of dendritic spines. Their data indicated that during early development, *Cdkl5*-null brains display significant reduction of spine density and PSD95-positive *puncta* when compared to WT littermates, whereas, the density of filopodia was similar between the two genotypes. These results suggested a potential involvement of Cdkl5 in the stabilization of mature mushroom-shaped spines rather than in the formation of new spines (*66*).

Another cytoplasmic substrate of CDKL5 is Amphiphysin 1 (AMPH1), a multifunctional adaptor molecule involved in neurotransmission and synaptic vesicles recycling through clathrin-mediated endocytosis. It has been demonstrated that CDKL5 phosphorylates AMPH1 on serine 293, negatively influencing its binding to endophilin, which is involved, among other processes that require remodelling of the membrane structure, in synaptic vesicle endocytosis and receptor trafficking. These evidence underlined once again how CDKL5 plays crucial roles in synaptic maintenance and function (*11*).

Recently, in our laboratory, it has been demonstrated that Cdkl5 deficiency in primary hippocampal neurons leads to deranged expression of the alpha-amino-3-hydroxy-5-

methyl-4-iso-xazole propionic acid receptors (AMPA-R). In particular, a dramatic reduction of expression of the GluA2 subunit was found concomitantly with its hyper-phosphorylation on Serine 880 and increased ubiquitination. These data also uncovered that *Cdkl5* silencing skews the composition of membrane-inserted AMPA-Rs towards the GluA2-lacking calcium-permeable form, which may contribute, at least in part, to the altered synaptic functions and cognitive impairment linked to loss of Cdkl5 (*12*).

Despite a clear involvement in shaping the dendritic arbour and synaptic spines, CDKL5 has been also shown to take part in the early phases of neuronal development. Indeed, Nawaz and colleagues highlighted the kinase in the regulation of proper axon specification and elongation in mouse primary hippocampal neurons: the silencing of *Cdkl5* resulted in an increased number of neurons bearing no axon, while both silencing and overexpression of the kinase were associated with the formation of supernumerary axons and reduced axonal length (*13*). These data were also strengthened by the identification of Shootin1 as novel CDKL5 interactor: indeed, Shootin1 is a brain-specific protein acting as a determinant of axon formation during the process of neuronal polarization. Importantly, silencing and overexpression studies have established that Shootin1 accumulation in the axon-to-be is both necessary and sufficient for axon outgrowth (*67*). These data reinforced the evidence that CDKL5 is involved in the regulation of neuronal polarization, al least in part, through its interaction with Shootin1.

Interestingly, Rac1, a Rho GTPase involved in the remodelling of actin and microtubule (MT) cytoskeleton, has shown to be common to the pathways of both CDKL5 and Shootin1. As a matter of fact, Shootin1 phosphorylation is induced by cdc42/Rac1-dependent Pak1 activation and CDKL5 has been reported to regulate neuronal morphology acting upstream Rac1 (*8*, *67*). Indeed, Chen and colleagues, using RNA-interfered rat cortical neurons, demonstrated that Cdkl5 localizes within F-actin in the peripheral domain of growth cones (GC) and interacts with Rac1 forming a protein complex that translocate to the membrane region in response to extracellular signals. Moreover, they found that this interaction is promoted by brain-derived neurotrophic factor (BDNF) (*8*). It is worth mentioning that mutations in members of Rho GTPase family have been identified in patients characterized by intellectual disability (*68*).

Recently, IQGAP1 has been identified in our laboratory as a novel CDKL5 interactor [Appendix 1, (*14*)]. IQGAP1 is the most studied of the three members of the IQGAP family of proteins, which are responsible for the regulation of several processes based on cytoskeletal remodelling, such as influencing migration and cell polarity, proliferation, cytoskeletal dynamics, vesicle transport and intracellular signalling through the interaction with numerous proteins (*69*). In particular, IQGAP1 regulates the correct interaction between microtubules and actin networks, through the formation of a triple complex (*15*) with activated Rac1 and CLIP-170, a plus-end microtubule binding protein that regulates microtubule stability plus acting as a rescue factor facilitating MT growth (*18*). We demonstrated that the loss of CDKL5 negatively impacts on the formation of such triple complex, which results in an alteration of IQGAP1 localization at the leading edge, a disruption of proper cell morphology and an impairment of CLIP-170 dynamicity.

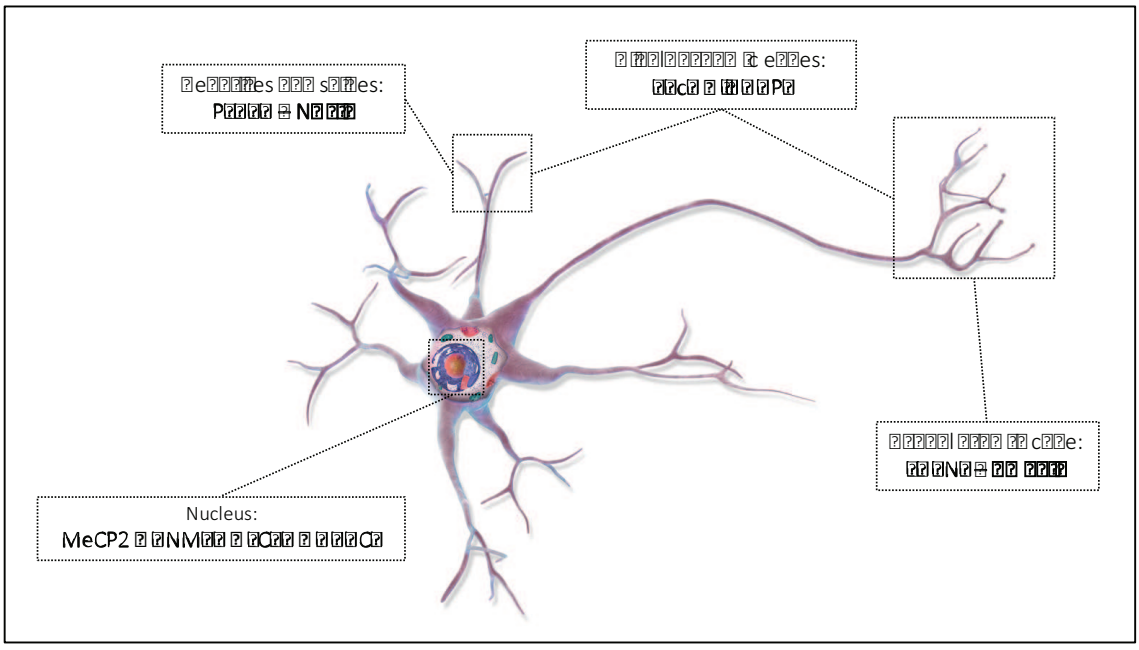

Fig. 1.10 Schematic representation of the localization of CDKL5 known interactors in neurons.

1.8 CDKL5 disorder animal models

Animal models are instrumental to understand the molecular mechanisms underlying the onset of a disease and, although they cannot summarize all aspects of a disorder, they generally represent an excellent tool to study gene functions. Thanks to the

development of *Cdkl5*-KO and conditional KO mouse models it has been possible to start understanding the roles of Cdkl5. The first *Cdkl5*-KO mouse model was generated by Wang and colleagues, reproducing a splice site mutation previously found in a CD patient (*70*). Thanks to the deletion of exon 6 of *Cdkl5* by homologous recombination in embryonic stem cells, they created a mouse model (background C57BL/6) with a truncation in the N-terminal domain of Cdkl5 disrupting the kinase activity. These animals showed autistic-like deficits in social interaction, as well as impairments in motor control (increased motor activity and altered motor coordination) and reduced learning and memory (*55*). Two years later, Amendola and colleagues produced a second mouse model, deleting *Cdkl5* exon 4 (background C57BL/6). This new model confirmed the behavioural defects characterized by Wang and collaborators, such as hind limb clasping and motor deficits, but also exhibited an impaired working memory phenotype. Altogether, these features mimic the impaired motor skills, reduced social interaction and intellectual disability observed in CD patients (*56*). Recently, a further characterization of a model generated by deleting exon 6 of *Cdkl5* (background C57BL/6), has been carried out by Zhang and colleagues. Several behavioural tests highlighted that the absence of Cdkl5 recapitulated the primary characteristics of autism and ADHD (Attention Deficit Hyperactivity Disorder), such as impaired social interaction, communication deficits and increase digging stereotypies, but also produced other symptoms like increased locomotion, impulsivity and aggressiveness, as well as deficits in motor and spatial learning (*71*).

To shed light on the cellular origin of distinct neuronal phenotypes conditional mouse models were developed. Amendola and colleagues generated two murine models carrying a Cre-conditional knockout (cKO) allele of *Cdkl5* with the specific deletion in forebrain GABAergic neurons (Dlx5/6::Cre mediated) or in cortical glutamatergic neurons (Emx1::Cre mediated), which revealed a double dissociation of behavioural phenotypes. Indeed, hind limb clasping defects and reduced head tracking response were only present in the Emx1-conditional *Cdkl5*-KO mice, while a decreased locomotion was characteristic of the Dlx5/6-conditional *Cdkl5*-KOs (*56*). Recently, a mouse model carrying the ablation of *Cdkl5* expression in forebrain glutamatergic neurons was generated. These animals showed a behaviour comparable with that of WT mice regarding basic sensory and motor function, anxiety and social behaviour,

whereas they displayed impairment in spatial working memory, increased locomotor activity and hind limb clasping (*72*).

Despite an extensive video-electroencephalography (EEG) monitoring, none of these models presented spontaneous epileptic seizures, a key phenotype in the human pathology. Nevertheless, Amendola and colleagues did observe an altered electroencephalogram response to a pro-convulsant treatment (kainic acid). Rather than increased seizure susceptibility the *Cdkl5*-KOs displayed a longer mean duration of seizures (35). Thus, the absence of an epileptic neuronal network suggests that the behavioural defects observed in these mice are the primary consequences of loss of Cdkl5. Recently, a KO mouse model (background C57BL/6N), generated by the deletion of *Cdkl5* exon 2 through Cre-LoxP recombination, showed significant hyperexcitability specifically to N-methyl-D-aspartate (NMDA). Indeed, these animals presented enhanced seizure susceptibility in response to NMDA, an up-regulation of NMDAR-mediated synaptic responses and a significant increase of GluN2B in the postsynaptic density (PSD) fraction. Based on these results the authors pointed out that the absence of Cdkl5 can give rise to epileptogenic propensity of KO mice due to the role of the protein in controlling the postsynaptic localization of GluN2B-containing NMDA receptor in the hippocampus (*73*).

Considering that the majority of CD patients are females with heterozygous *CDKL5* mutations, a detailed characterization of female heterozygous *Cdkl5* KO (*Cdkl5*$^{+/}$) mice emerged fundamental to advance preclinical and translational studies. In this regard, Fuchs and colleagues recently provided a behavioural and molecular analysis of female *Cdkl5*$^{+/-}$ mice (*Cdkl5* null strain in the C57BL/6N background developed in (*56*) and backcrossed in C57BL/6 for three generations): these females showed several aspects of CD, including autistic-like behaviour, motor impairment, learning and memory disability, and abnormal breathing pattern. Cdkl5 levels were found lower in the hippocampus and cerebellum, compared with the cortex, results that could explain the severe phenotypic outcome in hippocampus-dependent behaviours, more similar to homozygous *Cdkl5*-KO female and hemizygous *Cdkl5*-KO male mice. The heterozygous females mice also exhibited neuroanatomical defects, including dendritic hypotrophy and defects in spine density/maturation, altogether demonstrating that the

heterozygous females represent a valuable animal model for preclinical studies on CD (*74*).

1.9 Therapeutic strategies for CDKL5 disorder

At present, no cure exists for patients with CDKL5 disorder. However, in the last years, pharmaceutical targeting of deficient pathways in animal models of CDKL5 disorder has proven efficient in restoring some neuroanatomical and behavioural deficits in *Cdkl5*-KO mice.

As already described, loss of CDKL5 has been found to strongly affect the AKT/mTOR pathway. In 2015, Della Sala and collaborators demonstrated that treatment with IGF-1, an activator of this pathway, can rescue S6 phosphorylation, spine deficits, and PSD95 levels in *Cdkl5* KO mice. Of interest, these molecular alterations could not be linked to lower-than-normal levels of endogenous IGF-1, as cortical IGF-1 levels were normal. Importantly, IGF-1 administration was effective also in adult mice, when the synaptic deficit was already established and induced the formation of long-lasting spines (*66*).

A pharmacological intervention was also tested by Fuchs and colleagues, who demonstrated the efficacy of the modulation of the GSK3 pathway on hippocampal development and behavioural deficits in *Cdkl5*-KO mice. The SB216763-mediated inhibition of GSK3, which is hyperactivated when Cdkl5 is lacking, restored neuron survival and dendritic development, as well as spine morphology and distribution, and recovered the performance of *Cdkl5*-KO mice in hippocampus-dependent memory tasks. Moreover, one month after treatment withdrawal, the positive effects was still present, suggesting a long-term impact of the drug on such phenotypes (*75*). Interestingly, it has been recently demonstrated that, although GSK3 activity is impaired to the same extent in young and adult *Cdkl5*-KO mice, treatment with Tideglusib, another GSK3 inhibitor, improves hippocampal development only when the treatment is administered in the juvenile period and not in adulthood. These data suggest that a therapy with GSK3 inhibitors may be effective in CD patients only if administered early in postnatal development (*76*).

One year later, the targeting of HDAC4 was tested on *Cdkl5* KO mice; as mentioned, the activity of HDAC4 is altered in *Cdkl5*-KO mice, and considering that HDAC4 is involved in

memory formation, Trazzi and colleagues tested a drug known to inhibit HDAC4. Indeed, the treatment with LMK235 completely restored hippocampus-dependent memory in *Cdkl5*-KO mice. Unfortunately, it induced only marginal effects on hippocampal neuroanatomy, with a moderate increase in the number of new granule cells and their dendritic length. Previous findings showed that treatment with the pan-HDAC inhibitor VPA (valproic acid, a well-known anti-epileptic drug) has negative effects on the proliferation of adult hippocampal neural progenitor cells, and that prenatal exposure impairs hippocampal function. Moreover, several clinical studies have demonstrated that pan-HDAC inhibitors may cause a plethora of side effects, including bone marrow depression, diarrhoea, weight loss and cardiac arrhythmias. This evidence indicates the need of targeted inhibitors, which modulate specific HDACs, thus reducing the off-target effects produced by unspecific inhibition. In this regard, the treatment with LMK235 demonstrated to have a positive impact on hippocampal development and function with no adverse effects on the well-being of animals (*7*).

Lately, in our laboratory Pregnenolone has been found to have positive effects on CDKL5-related morphological defects both in cycling cells and in neurons [Appendix 1, (*14*)]. P5 is an endogenous steroid generated from cholesterol by the action of CYP11A1 and it is known to bind and activate CLIP-170, an interactor of IQGAP1, by changing its conformation and potentiating its ability to enhance microtubule assembly and interaction with microtubules and the microtubule-associated proteins, processes which have been found altered in CDKL5-lacking cells (*21*).

Very recently, we also demonstrated that Tianeptine, a cognitive enhancer and antidepressant drug, known to recruit and stabilise AMPA-Rs at the synaptic sites, is capable of normalising the expression and membrane insertion of AMPA-Rs as well as the number of PSD95 clusters. Indeed, Tianeptine treatment normalized GluA2 expression in *Cdkl5* silenced neurons (*12*). Of relevance, in a previous study Tianeptine was found capable of improving the respiration phenotype in a mouse model of RTT (*77*), making this drug an interesting candidate for the treatment of CD.

While these data raise hope that pharmaceutical intervention is possible for CDKL5 disorder, the field still needs to further disentangle the networks regulated by CDKL5 to provide the basis for the rationale design of therapeutic strategies.

1.10 Neuronal microtubule dynamics and MT-related drugs

Considering the high complexity of the nervous system, it is evident that sophisticated cytoskeleton-based processes are required to coordinate the proliferation, migration, and differentiation of neurons. The structural organization and dynamic remodelling of the neuronal cytoskeleton contribute to all the morphological and functional changes in neurons. Along with the actin cytoskeleton, the assembly, organization and remodelling of MTs are essential to successfully complete all the different stages of neuronal development (*78*).

MTs switch between phases of growth and disassembly in a process named dynamic instability, which allows individual MTs to explore cellular regions and retract in case they do not find the proper environment. MT dynamics are mainly regulated by +TIPs, which accumulate at the ends of growing MTs and control different aspects of neuronal development and function (*79*). Such dynamicity requires also the coordinated actions of many additional regulatory factors such as neuron specific tubulin isotypes, post-translational modifications (PTMs), motor proteins, and various microtubule-associated proteins (MAPs) (*80*, *81*). Neuronal MTs guide intracellular transport and induce morphological changes during the various phases of neuronal development and synapse formation. The extreme dimensions of neurons necessitate active transport mechanisms to properly distribute many different cellular components and to establish robust signalling pathways from the synapse to the soma and vice versa (*82*). MTs also play important roles during the morphological transitions that occur during neuronal development, such as neurite initiation, migration, polarization, and differentiation, contributing to these processes by facilitating transport to specific sites, by providing mechanical forces, or by acting as local signalling platforms (Fig.1.11).

Neuronal migration is promoted by actin dynamics undergoing protrusive polymerization at the leading edge and propulsive contractions at the cell rear. The MT cytoskeleton in migrating neurons is anchored to the centrosome, extends into the leading edge, and forms a cage-like structure around the nucleus. Cytoskeletal forces at the tip of the leading edge may then pull the centrosome into the proximal part of the leading process, thereby moving the nucleus in the direction of migration (*83*). Furthermore, a complex remodelling and reorganization of MTs occur in the growth

cone during axon elongation (*84*): MTs participate in functional interactions with adhesion complexes, actin and numerous +TIPs. In addition to MT assembly, translocation of the whole MT bundle in the axon may contribute to axon elongation (*85*). The MT cytoskeleton also contributes to neurite outgrowth: indeed several studies have demonstrated that both MTs and actin filaments mediate the pushing and pulling forces that contribute to membrane protrusion, combining a local increase in actin dynamics and a MT stabilization (*16*, *84*). Moreover, such stabilization plays a key role in the initial specification of the axon during neuronal polarization (*79*).

Finally, MTs play a central role in the structural changes of dendritic spines. (*86*). Current evidence suggests that MT entry is associated with transient changes in spine shape, such as the formation of spine head protrusion and spine enlargement (*79*). Although not demonstrated directly, it is likely that microtubule-dependent motors use dynamic MT entries to drive postsynaptic cargos into spines.

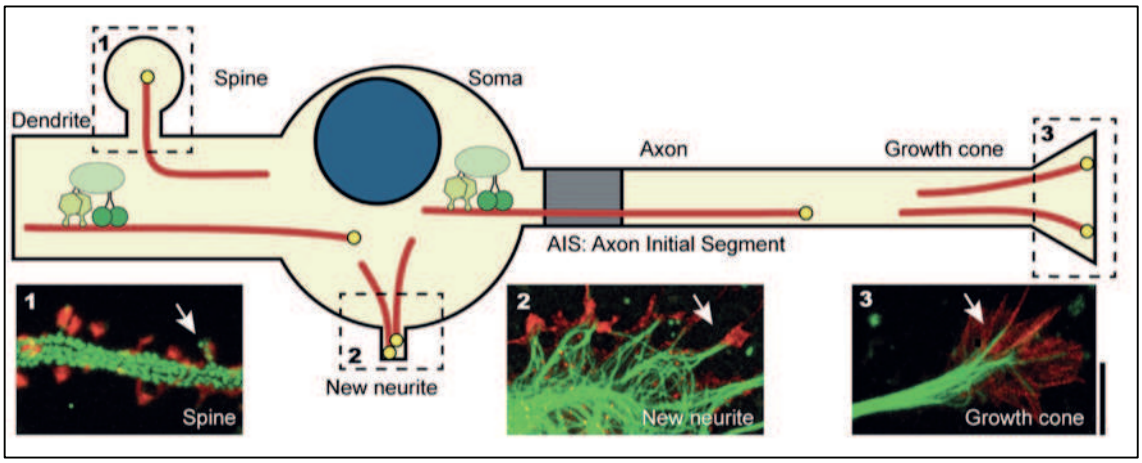

Fig. 1.11 MTs in neurons. Cartoon illustrating the different functions of neuronal microtubules. Zooms show microtubule organization in dendritic spines (1), emerging neurites (2), and growth cones (3) of cultured rat hippocampal neurons (*87*).

Reflecting the importance of the MT cytoskeleton in neuronal development, MT defects cause a wide range of nervous system abnormalities and several human neurodevelopmental disorders have been linked to altered microtubule-mediated processes. Mutations in microtubule-related genes encoding MAPs (e.g. Tau), MT severing proteins (e.g. spastin), microtubule-based motor proteins (e.g. dynein, kinesin), and motor associated regulators (e.g. dynactin, doublecortin, and lis1) are associated

with various neurodevelopmental problems (*88*, *89*). In addition, impairment of axonal transport in mature neurons is a common factor in many of the major neurodegenerative diseases, including the motor neuron diseases amyotrophic lateral sclerosis (ALS) and Alzheimer's disease (*90*) and neuroinflammatory diseases such as multiple sclerosis (*91*).

Considering all above, in the last years, drugs acting on MTs have been proposed for the therapy of several neurodevelopmental and neuropsychiatric disorders, including autism, schizophrenia, and depression mainly due to their stabilizing properties, aiming to restore neuronal axonal transport and reduce tau phosphorylation.

Epothilone D (EpoD) is a taxol-related compound that interacts directly with tubulin to stabilize MTs and is currently used in clinical trials for the treatment of various tumors. However, at nanomolar concentrations, this compound improves MTs density and axonal transport, reduces axonal dystrophy and enhances cognitive performance, without notable effects on viability and development in mouse (*92*).

Non-taxane MTs stabilizers such as NAP and all D-SAL have been found to be effective in the treatment of schizofrenia. Such compounds, interactng with the microtubule binding protein EB3, showed a neuroprotective activity (*93*). NAP was also found to enhance Tau-MTs binding under stress conditions and stimulated axonal transport (*94*, *95*).

Risperidone is a second-generation antipsychotic drug, which, besides its function on dopamine and serotonin receptors, was found to interact with the EB1-EB3 protein family and to compete with NAP binding on EB3. Risperidone improves the neurocognitive functions in patients with schizophrenia (*96*) and is used in autistic patients for the treatment of associated symptoms as disruptive behaviour and hyperactivity (*97*).

Currently several compounds have been proposed for the therapy of numerous neurodevelopmental disorders mainly due to their potential as MT modulating agents.

One of these compounds is melatonin, a hormone involved in the regulation of circadian rhythms, blood pressure, seasonal reproduction (*98*). Melatonin is capable of increasing MAP2 levels thus increasing MT polymerization and dendrite stabilization (*99*). Several data support the potential use of melatonin as MT stabilizing agents in the

treatment of depression and anxiety associated to schizophrenia (*100*).

Other interesting compounds are synthetic or non-synthetic neurosteroids. The synthetic MT-associated protein/neurosteroidal pregnenolone, PME, has been studied in the context of schizophrenia-associated depression to prevent branching reduction and synaptic contact loss (*22*). In rodents PME was able to protect them from developing a depressed state. Furthermore, it prevented the loss of □-tubulin acetylation and sleep disturbances following psychosocial stress (*101*). By binding MAP2, PME stimulates MT assembly and promotes neurite growth (*102*).

Also lithium can act on MTs and have a beneficial role in cytoskeleton regulation in mood disorders. Indeed, it has been shown to act as a GSK3□ inhibitor, thus decreasing phosphorylation of tau and MAP1B finally leading to MTs remodelling (*103*).

MT targeting therapies could be able to improve or even prevent some structural and functional alterations linked to neurodevelopmental disorders. Currently only few of these compounds have been tested on humans in clinical trials but increasing number of new drugs are being tested in experimental studies in both □*in vitro* and □*in vivo*. The possibility to act on MTs for pharmacological intervention in neurological diseases is progressively becoming a solid opportunity.

2. Aim

Although there have been important steps towards an increased knowledge of CDKL5 functions, its roles are still not fully understood. Its localization in both the nucleus and the cytoplasm of expressing cells suggests that it may be involved in several cellular processes. Among other functions, CDKL5 is known to regulate cellular morphology through its interacting proteins. Our recent publication demonstrated that IQGAP1, a novel CDKL5 interactor, and its binding partners CLIP-170 and Rac1, in absence of CDKL5 display altered localization and dynamics in cells [Appendix 1, (*14*)]. Indeed, we found that CDKL5 regulates cytoskeletal dynamics enhancing Rac1–IQGAP1–CLIP-170 complex formation and promoting CLIP-170 dynamics on MTs.

Starting from such results, we firstly decided to investigate the potential role of CDKL5 in the specific regulation of CLIP-170. CLIP-170 is a MT plus end tracking protein (+TIP) that is known to coordinate cytoskeletal dynamics bridging actin cytoskeleton and microtubules and promoting MT growth (*18*). Considering that CLIP-170 alternates between a folded inactive conformation, in which it cannot interact with MTs and other proteins, and an open extended conformation, which allows its binding to MTs and other interacting proteins (*19*), we firstly envisaged that CDKL5 could have a role in the regulation of CLIP-170 conformational state stabilizing its extended conformation and increasing its binding to MTs.

Once assessed that the loss of CDKL5 impairs CLIP-170 activity, increasing its inactive state, we hypothesized that Cdkl5 may exert a similar role in primary hippocampal neurons. Indeed, drawing an analogy with cells, we characterized neuronal morphological phenotypes, which may be altered in *Cdkl5*-KO neurons via CLIP-170, and investigated the presence of CLIP-170 at such level. At early developmental stages we analysed axonal phenotypes, such as axon specification and elongation, and at late stages dendritic phenotypes, such as spine formation, morphology and maturation. These phenotypes had been already found altered in *Cdkl5*-silenced neurons and in null brains (*7*, *9*, *10*, *13*, *66*, *75*). Moreover, we analysed MT organization at the growth cone level, considering that CLIP-170 role at such level has been already proven (*16*).

To corroborate our hypothesis of CLIP-170 role in the regulation of such phenotypes in

Cdkl5-null neurons, we investigated its presence at such level. The identification of the +TIP at the growth cone level strengthen our data on axonal altered phenotypes, while the detection of CLIP-170 in spines shed light on a potential novel role of such protein at this level.

Eventually, we evaluated the effects of the two compounds Pregnenolone and its syntactic derivative PME on the defective phenotypes found in neurons and cycling cells. P5 has already demonstrated to be effective in ameliorating CLIP-170 dynamics on MTs in CDKL5-depleted cells and in correcting altered axonal phenotypes in Cdkl5-silenced primary hippocampal neurons [Appendix 1, (*14*)]. This neurosteroid was recently identified as modulator of CLIP-170 activity. Indeed, by binding this +TIP, P5 induces its active conformation and promotes its interaction with MTs, allowing MT polymerization (*21*). Considering that P5 is an endogenous neurosteroid, which gets converted into its downstream metabolites and considering the possible side effects of P5 metabolites in a future clinical application of such compound, we decided to evaluate alongside the effects of its non-metabolizable derivative PME (*22*) on *Cdkl5*-KO neurons and CDKL5-depleted COS7 cells.

In summary, the aim of this study has been to investigate the potential role of CDKL5 in the regulation of the +TIP CLIP-170, through a functional analysis using FRET assay and a morphological characterization of *Cdkl5*-KO neurons. Moreover, our intent has also been to evaluate the potential effects of the compounds P5 and PME on the altered CDKL5-related morphological defects found in cells and neurons.

3. Materials and methods

3.1 Ethical statement

Protocols and use of animals were approved by the Animal Ethics Committee of the University of Insubria and in accordance with the guidelines released by the Italian Ministry of Health. Adult mice were euthanized by cervical dislocation, while neonates were sacrificed by exposure to CO_2 followed by decapitation.

3.2 Plasmids

mEmerald-CLIP170-N-18 (plasmid 54044; Addgene; GFP–CLIP-170). YFP-CLIP-170-CFP has been kindly provided by the Anna Akhmanova laboratory. The construct was derived from the GFP-CLIP-170 fusion, based on the rat brain CLIP-170 cDNA. To make this construct, the GFP was substituted for YFP, and the monomeric (A206K) CFP, preceded by a 7–amino acid linker, was fused to the end of the CLIP-170 ORF using a PCR-based strategy (*19*).

3.3 Antibodies and reagents

The following primary antibodies (Abs) were used for immunofluorescence and western blotting experiments: anti-CDKL5 (Sigma-Aldrich, HPA002847; Santa Cruz, sc-376314), anti-CLIP170 (Genetex, GTX117504; Santa Cruz H-300, sc-25613), anti-Tau1 (Millipore, MAB3420), anti-MAP2 (ab32454, Abcam), anti-PSD95 (Thermo Fischer Scientific, MA1045), anti--tubulin (Sigma-Aldrich, T6074), anti-GAPDH (Sigma-Aldrich, G9545), anti-GFP (Roche, 1814460). Phalloidin-TRITC Conjugates (Sigma-Aldrich P1951). HRP-conjugated goat anti-mouse or anti-rabbit secondary Abs for immunoblotting, DAPI, and secondary Alexa Fluor anti- rabbit and anti-mouse Abs for immunofluorescence (IF) were purchased from Thermo Scientific.

3.4 Cell cultures

COS7 cells were maintained in DMEM (Dulbecco's modified Eagle's medium; Sigma-Aldrich) supplemented with 10% FBS (EuroClone), L-glutamine (2mM, EuroClone), penicillin/streptomycin (100 units/mL and 100 μg/mL respectively, EuroClone) at 37°C with 5% CO_2.

For siRNA transfection, cells were cultured in 6- or 24-well dishes and 20nM siRNA oligonucleotides targeting CDKL5, or a control siRNA (siCDKL5 5'GCAGAGTCGGCACAGCTAT3', siCtrl 5'CGUACGCGGAAUACU UCGATT3') were transfected using Lipofectamine™ RNAiMAX (Life Technologies Incorporated). For plasmid transfection, Lipofectamine™ 3000 (Life Technologies Incorporated) was used.

3.5 Primary neuronal cultures

Primary hippocampal cultures were prepared from brains of CD1 mouse embryos at embryonic day 17 (E17) considering the day of the vaginal plug as E0. Wild-type and *Cdkl5*-null embryos were obtained from pregnant heterozygous females (*Cdkl5*$^{-/+}$, CD1 background) crossed with wild-type males. The mice were sacrificed by cervical dislocation and the embryos were recovered and hippocampi rapidly dissected. After washing in HBSS (Gibco), the hippocampi were dissociated by 7 min incubation at 37°C in 0.25% trypsin (Sigma-Aldrich) and further washed in HBSS. Neurons were suspended in Dissecting Medium [DMEM (Sigma-Aldrich), 10% horse serum (EuroClone), 2 mM glutamine (EuroClone), 1 mM Sodium Pyruvate (Gibco)] to block the action of trypsin. Eventually, cells were mechanically dissociated by pipetting and plated on coverslips coated with poly-L-lysine (1 mg/mL, Sigma-Aldrich) or poly-D-lysine (Neuvitro) in 24-well plates (densities: $3.75x10^3/cm^2$ for immunostaining and $1.2x10^4/cm^2$ for western blots); neurons were maintained in Neurobasal medium (Gibco) supplemented with 2 mM GlutaMAX™ Supplement (Gibco) and 2% B27 (Gibco) in a humified incubator with 5% of CO_2 at 37°C. After 3 days in vitro, cytosine-1-β-D-arabinofuranoside (Sigma-Aldrich) was added to cultured neurons at final concentration of 2 μM to prevent astroglial

proliferation. Transfection of hippocampal neurons was performed by adding a GFP-expressing vector 11 days after plating to visualize neuronal architecture.

3.6 Immunofluorescence

After fixation in 4% paraformaldehyde (Thermo Fischer) with 4% sucrose (Sigma-Aldrich) neurons were blocked in PBS (EuroClone) with 5% horse serum, 0.2% Triton X-100 (Sigma-Aldrich) before incubation with the appropriate primary antibodies overnight at 4°C and subsequently with the secondary antibodies for 1 hour at room temperature. Slides were mounted with ProLong Gold antifade reagent (Life Technologies).

3.7 Drug preparation

Pregnenolone (P5 or 3β-Hydroxy-5-pregnen-20-one) was purchased from Sigma-Aldrich and dissolved in 100% EtOH (Sigma-Aldrich). Its synthetic derivative, PME (Pregnenolone-Methyl-Ether, 3β-methoxy-pregnenolone, MAP4343 or MePreg), was kindly synthesized and provided by Transpharmation Ltd and dissolved in 100% DMSO (Sigma-Aldrich). Progesterone (P4 or 4-Pregnene-3,20-dione) was purchased from Sigma-Aldrich and dissolved in water.

3.8 Measurement of comet length and lifetime

For time-lapse imaging COS7 cells were transfected with the indicated siRNAs (siCDKL5 and siCTRL) and 60 hours later with pGFP-CLIP170; microscopy analysis was performed after another 24h. Pharmacological treatment was performed incubating cells with PME 1 μM or with 0.001% DMSO (Sigma-Aldrich) as control vehicle for three days (starting treatment 24 h after siRNA transfection).

Fluorescence in the specimens was imaged every 3 seconds for 3 min with a confocal laser-scanning microscope (model TCS SP8; Leica) with a 63X NA 1.2 oil immersion

objective (Leica). Comet length and life-time were analysed using the tracking function of the MTrack plug-in of Image software.

3.9 FRET measurement

For FRET measurements COS7 cells were seeded in a 6-well plate with glass coverslips (density: 5000 cells/cm2), transfected with the indicated siRNAs (siCDKL5 and siCTRL) and 24 hours later with YFP-CLIP-170-CFP; 24 hours after silencing, cells had been left untreated or treated daily with 1 M P5, PME or the respective vehicles (0.0032% EtOH and 0.001% DMSO, Sigma-Aldrich). Microscopy was performed 72 hours after silencing. Images were obtained by an inverted point scanning confocal Leica SMD SP8 (Leica Microsystems) with a 63X/1.4 objective with the LASX software and the module of FRET Sensitized Emission (excitation at 458 nm) at 37 C. FRET efficiency of at least 10 cells per condition was calculated as the ratio between the FRET signal/donor signals using the LASX software.

3.10 Analysis of growth cone

To analyse growth cone area and CLIP-170 localization at the tip of the axon the Image software was used. WT and KO hippocampal neurons were maintained in conditioned medium and left untreated or treated at DIV1 for 48 hours with the following compounds: 1 M P5, 1 M PME or 1 M P4 or with vehicles (0.0032% EtOH or 0.001% DMSO).

To calculate the growth cone area, a fixed area of 18x18 m^2 starting from the most distal MT tip towards the axon shaft was outlined manually. The MT area was then quantified using the -tubulin stained region within the selected area. To analyse the localization of CLIP-170 at the growth cone site, a fixed area of 25x25 m^2 starting from the edge of actin cytoskeleton towards the axon shaft was outlined manually. The ratio of CLIP-170 versus -tubulin was determined from fluorescence areas of both channels; the fold change value was used as measure of CLIP-170 distribution. Growth cone morphology was analysed by staining with -tubulin. Growth cones were classified as

“extending” or “paused”: growing growth cones characterized by straight bundles of MTs projecting outward into actin lamellipodium were considered as “extending”; whereas, large growth cones with MTs organised in the central region as a prominent loop were considered as “paused” (*104*).

3.11 Analysis of neuronal polarization and axon length

WT and KO hippocampal neurons were maintained in conditioned medium and treated at DIV1 (DIV: days in vitro) for 72 hours with the following compounds: 1 µM P5, 1 µM PME or 1 µM P4 or with vehicles (0.0032% EtOH or 0.001% DMSO, Sigma-Aldrich).

Neuronal polarization was analysed at DIV4 by staining with the axonal marker Tau1. Neurites with a significant intensity of Tau-1 staining increasing along the proximal to distal axis were counted as axons. Neurons were classified as polarized (one axon) or unpolarised (either lacking an axon or with multiple axons). Axon length was analysed with ImageJ using the NeuronJ plugin to compute the path from the beginning to the end of the axon.

3.12 Analysis of PSD95 *puncta*, spine density and morphology

Cdkl5-WT and KO hippocampal neurons were maintained in conditioned medium and treated from DIV11 for 72 hours with the following compounds: 1 µM P5, 1 µM PME or 1 µM P4 or with vehicles (0.0032% EtOH or 0.001% DMSO, Sigma-Aldrich).

PSD95 *puncta* were analysed at DIV15 by staining with antibodies against the postsynaptic density protein 95 (PSD95) and MAP2 to visualize mature spines and neuronal dendrites, respectively. The number of PSD95 *puncta* was measured in 5-10 dendrites of 30 µm per condition using the software ImageJ (function: Analyse particles).

Spine density and morphology were analysed thanks to the software Neuron Studio. Firstly, 50 spines were loaded in the software as reference: the software generated an algorithm that was used for the following analysis. Thanks to this setting, the program

was able to divide spines in four different classes: mushroom, thin, filopodia and stubby. 5/10 dendrites of around 30 µm per condition were analysed.

3.13 Western blotting

COS7 cells were directly lysed with Laemmli buffer 2X (120 mM Tris-HCl pH 6.8, 4% SDS, 20% Glycerol (Sigma-Aldrich), 0.02% Bromophenol blue), sonicated and boiled (5', 95°C). Samples were separated by 10% SDS-PAGE, transferred to nitrocellulose membranes, and blocked in 5% non-fat milk in TBS [20 mM Tris-HCl pH 7.5, 150 mM NaCl (Sigma-Aldrich)] with 0.2% Tween-20 (Sigma-Aldrich), TBS-T. Blots were incubated with primary antibodies overnight at 4°C, washed in TBS-T, and incubated with appropriate secondary antibodies for 1h at room temperature. After extensive washes, blots were developed with Protein Detection System-ECL (Genespin).

3.14 Synaptosomal fractionation

CD1 mouse hippocampi were homogenized using a tissue grinder in homogenization buffer [320 mM sucrose (Sigma-Aldrich), 5 mM sodium pyrophosphate (Sigma-Aldrich), 1 mM EDTA (Sigma-Aldrich), 10 mM HEPES (Sigma-Aldrich), pH 7.4, and protease inhibitor mixture (Roche)]. The homogenate was then centrifuged at 800 × g for 10 min at 4 °C to yield P1 (nuclear fraction) and S1 fractions. S1 fraction was further centrifuged at 17000 × g for 20 min at 4 °C to yield P2 (membrane/crude synaptosome) and S2 (cytosol) fractions. P2 was resuspended in homogenization buffer and layered onto nonlinear sucrose gradient cushion (1.2 M, 1.0 M, and 0.8 M sucrose from bottom to top), then centrifuged at 82.500 × g for 2 h at 4 °C. Synaptosomes were collected at the interface of 1.0 M and 1.2 M sucrose cushion. Collected synaptosomes were diluted with 10 mM HEPES, pH 7.4, to reach a final concentration to 320 mM sucrose and then centrifuged at 150,000 × g for 30 min at 4 °C. The final synaptosome pellet was resuspended in 50 mM HEPES, pH 7.4, followed by protein quantification and biochemical analysis.

3.15 Data analyses

Data quantification, including cell migration, comet length and lifetime, and protein interaction were analyzed with Prism software (GraphPad) and are shown as mean SEM. Two-tailed Student's t-test or ANOVA were used for statistical analyses. Probability values of P 0.05 were considered as statistically significant.

3.16 Nomenclature

CDKL5 written in upper case letters refers to the human protein, whereas Cdkl5 in lower case letters refers to the murine counterpart. *CDKL5* and *Cdkl5* reported in italics indicate the human and the murine genes, respectively.

4. Results

4.1 The loss of CDKL5 alters the conformational state of CLIP-170

Previous results obtained in our laboratory demonstrated that the loss of CDKL5 leads to impaired MT dynamics probably due to the delocalization of IQGAP1 and the impairment of CLIP-170 dynamicity on MTs [Appendix 1, (*14*)]. In vitro studies have demonstrated that CLIP-170 activity is tightly regulated by its specific conformation: through an interaction between its NH_2- and COOH-termini CLIP-170 alternates between an active, extended conformation, in which it can interact with MTs and its COOH-terminal partners, and an inactive, folded conformation, blocking its association with other proteins (*19*). As mentioned, our published results demonstrated that the absence of CDKL5 leads to a reduced affinity of CLIP-170 for MTs (*21*), suggesting that it might play a role in regulating CLIP-170 functioning by altering its conformation.

Considering all above, we decided to evaluate if CDKL5 could influence, directly or indirectly, the conformational state of CLIP-170. To address this, we analysed the intramolecular state of CLIP-170 by fluorescence resonance energy transfer (FRET) analysis. To monitor protein conformational changes with the FRET technique, the target protein is labelled with fluorescent donor and acceptor molecules at the two extremes. When the donor (Cyan Fluorescent Protein, CFP) and the acceptor (Yellow Fluorescent Protein, YFP) are in proximity (1-10 nm) due to the interaction of the two tagged domains, the acceptor emission intensity increases because of the intramolecular FRET from the donor to the acceptor (the emission spectrum of CFP and the excitation spectrum of YFP overlap between 450 and 550 nm). Thus, we expressed a YFP-CLIP-170-CFP fusion protein in COS7 cells after the silencing of CDKL5 expression (siCDKL5) (Fig.4.1C). The FRET efficiency, calculated as FRET signal to CFP (donor) fluorescence ratio (FRET/donor), was examined in vivo by live microscopy acquisition at 37°C.

As shown in fig. 4.1 A-B, we observed a higher FRET efficiency in siCDKL5 cells compared to control (siCTRL) cells (siCRTL: 50.81% ± 3.23; siCDKL5: 74.39% ± 3.71), indicating that in the absence of CDKL5, CLIP-170 is mainly present in a closed conformation. This

result is in line with the reduced affinity of CLIP-170 previously observed in CDKL5 silenced cells.

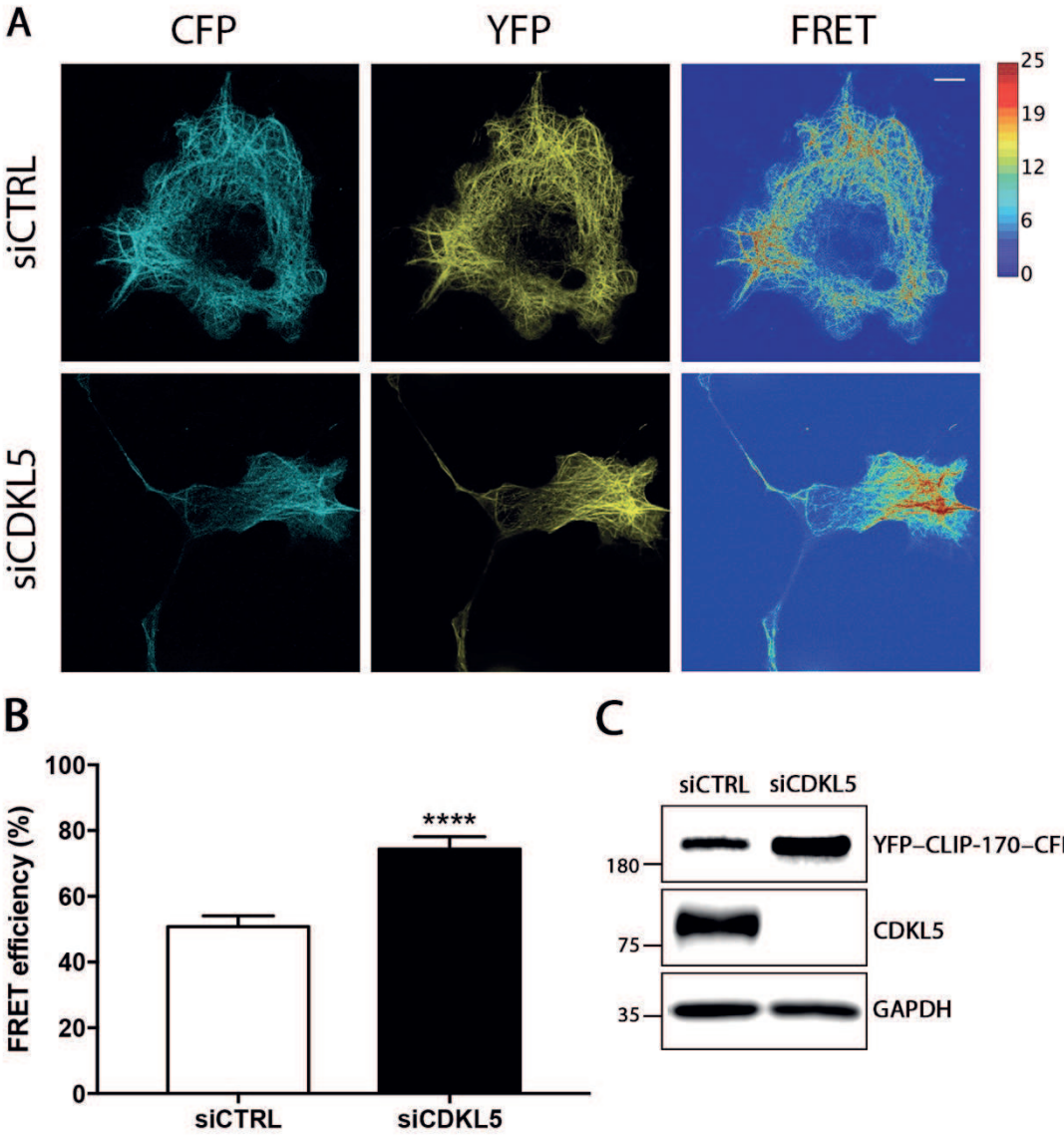

Fig. 4.1 CDKL5 influences the conformational state of CLIP-170. (A) Representative images of COS7 cells transfected with a YFP–CLIP-170–CFP expressing vector 72 h upon silencing with siCDKL5 or siCTRL. The columns show CFP and YFP images as indicated, the third column shows a pseudo-colour rendering of the FRET signal. Calibration bar indicates the intensity of the FRET signal, with red colour representing a high FRET signal. Scale bar, 10 m. (B) Graph showing the mean percentage of FRET efficiency in siCDKL5 compared to control cells. Data information: data are shown as mean SEM (P 0.0001), Student's t-test. At least 25 cells for each condition were analysed from three independent experiments. (C) COS7 cells were treated as in A. CDKL5 and YFP–CLIP-170–CFP levels were analysed by WB using antibodies against CDKL5 or GFP, respectively. GAPDH was used as loading control.

4.2 Cdkl5-KO neurons show altered growth cone morphology

MTs play a crucial role in neuronal polarization by sustaining the transport of proteins and organelles for axon formation. Recently, we demonstrated that primary hippocampal neurons silenced for Cdkl5 are characterized by defective axon formation and outgrowth (*13*). Interestingly CLIP-170, as well as CDKL5, positively regulates axon dynamics. In particular it has been demonstrated that a hypo-functional CLIP-170 derivative impaired growth cone morphology and axon outgrowth (*16*). The growth cone is an expanded, motile structure at the tip of the axon that is divided into several distinct regions: the central region is characterized by an enrichment of MTs, while the most peripheral domain is mainly composed of actin filaments. The junction between the central domain and the peripheral region is the transition zone, in which MTs protrude during axonal extension (*105*). A correct cytoskeletal organization of such structure plays an important role in axon outgrowth (*84*). In light of the above data, we speculated that the axonal defects linked to Cdkl5 deficiency could be due to a deranged MT organization in the axonal growth cone. For this purpose, we analysed the distribution of MTs at the tip of the axon of *Cdkl5*-WT and KO primary hippocampal neurons at DIV3. Firstly, we calculated the growth cone area quantifying □-tubulin staining within a fixed area. We found that growth cones of *Cdkl5*-KO neurons were significantly enlarged from 41.75□m^2□2.15, in control cells, to 71.26□m^2□1.91, corresponding to a 1.71-fold increase (Fig. 4.2 A and B).

It has been demonstrated that the growth cone size inversely correlates with axonal growth rate: indeed, growth cones at the tip of rapidly extending axons are typically small, straight and characterized by highly motile MTs. Conversely, in slowly growing axons, MTs become bundled and form loops that cause an enlargement of the structure. In the latter situation the growth cone is called "paused□ because it maintains its motility without advancing forward (*104*, *106*). Considering that the loss of Cdkl5 reduces axon elongation, we evaluated whether *Cdkl5*-KO growth cones display a paused phenotype compared to that of the WT controls. As shown in fig. 4.2 C and D, axonal growth cones of DIV3 *Cdkl5*-null neurons are mostly characterized by markedly looped MT structures corresponding to a paused state (WT: 8%□4.9; KO: 37,33%□8,03).

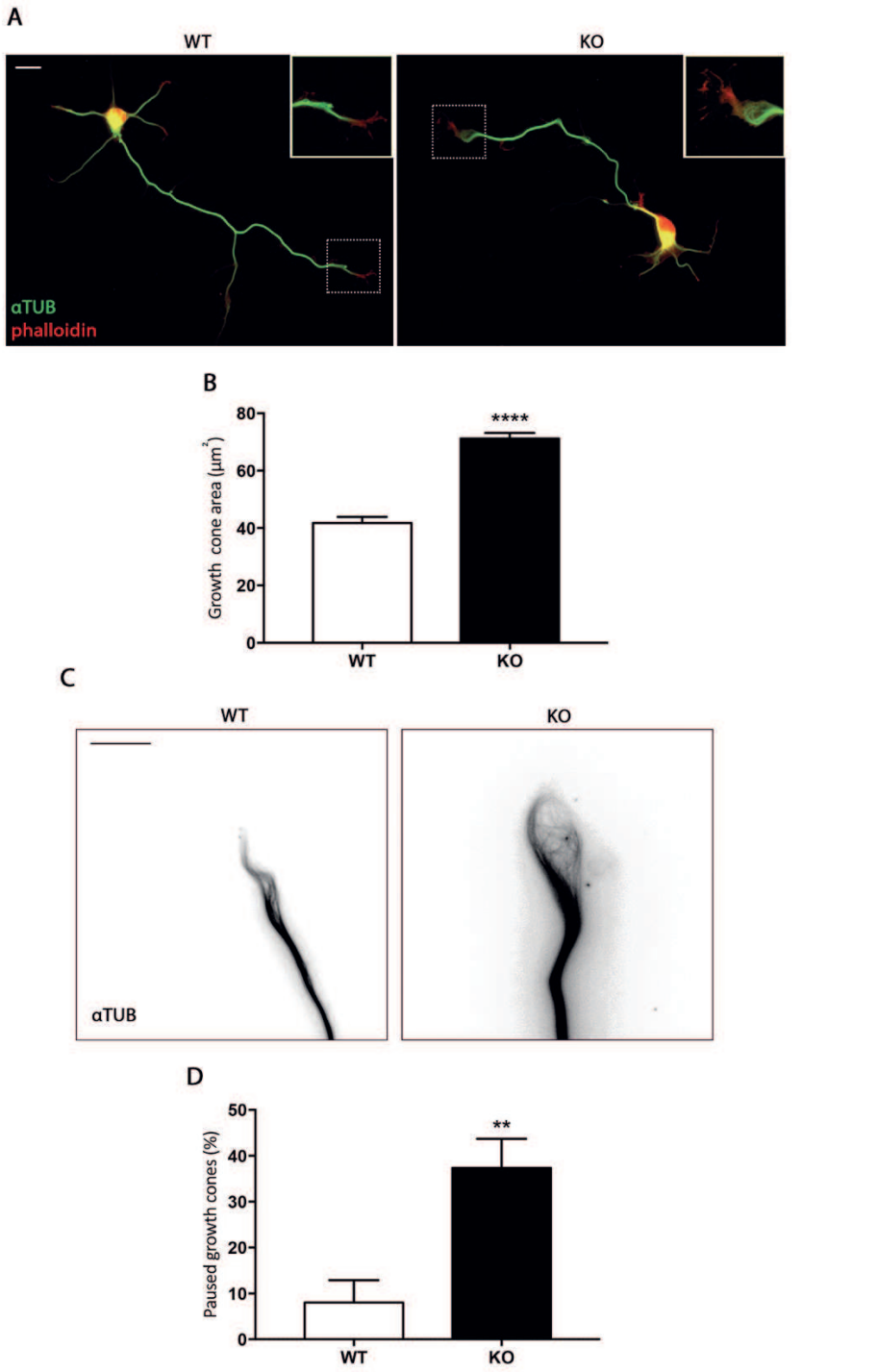

Fig. 4.2 *Cdkl5*-KO axonal growth cones show an enlarged MT area and a paused phenotype. (A) Representative images of WT and *Cdkl5*-KO hippocampal neurons (DIV3) stained for -tubulin (green) and phalloidin (red) to visualize microtubules and actin, respectively (scale bar, 10 m). The boxed areas are magnified to the right. (B) Graph showing the mean microtubule area in growth cones quantified as described in Materials and methods. Data information: data in B are presented as mean SEM (P0.0001), Student's t-test. At least 100 neurons for each genotype were analysed from six independent neuronal preparations. (C) Representative images of WT and *Cdkl5*-KO hippocampal neurons (DIV3) stained for -tubulin visualize straight or looped microtubules (scale bar, 5 m). (D) Graph showing the mean percentage of paused growth cones quantified as described in Materials and methods. Data information: data in D are presented as mean SEM (P0.01), Student's t-test. At least 50 neurons for each genotype were analysed from three independent neuronal preparations.

4.3 Cdkl5 regulates CLIP-170 localization at the growth cone level

It has been demonstrated that CLIP-170 localizes at the level of the growth cone in both axons and minor neurites, influencing their proper development and elongation (*16*, *17*). Therefore, considering our results indicating a role of CDKL5 in regulating the activity of CLIP-170, we speculated that the CDKL5-dependent impairment of CLIP-170 functioning could affect its proper localization at the growth cone. Thus, by immunocytochemistry we analysed the localization of CLIP-170 in growth cones of *Cdkl5*-WT and KO DIV3 primary hippocampal neurons. Neurons were stained against CLIP-170 together with □-tubulin and phalloidin (to visualize the entire growth cone area) and the ratio between the areas of CLIP-170 and □-tubulin was measured within a selected region of interest (Fig. 4.3 A). We found that CLIP-170 co-localized with □-tubulin in the majority of *Cdkl5*-WT neurons. By contrast, in *Cdkl5*-null neurons CLIP-170 was distributed within the entire growth cone area as shown in fig. 4.3 A-B and in the schematic model (Fig. 4.3 C), suggesting that a reduced number of CLIP-170 molecules was bound to MTs in absence of Cdkl5 (CLIP-170/tubulin ratio: WT: 1.1□0.09; KO: 1.65□0.15).

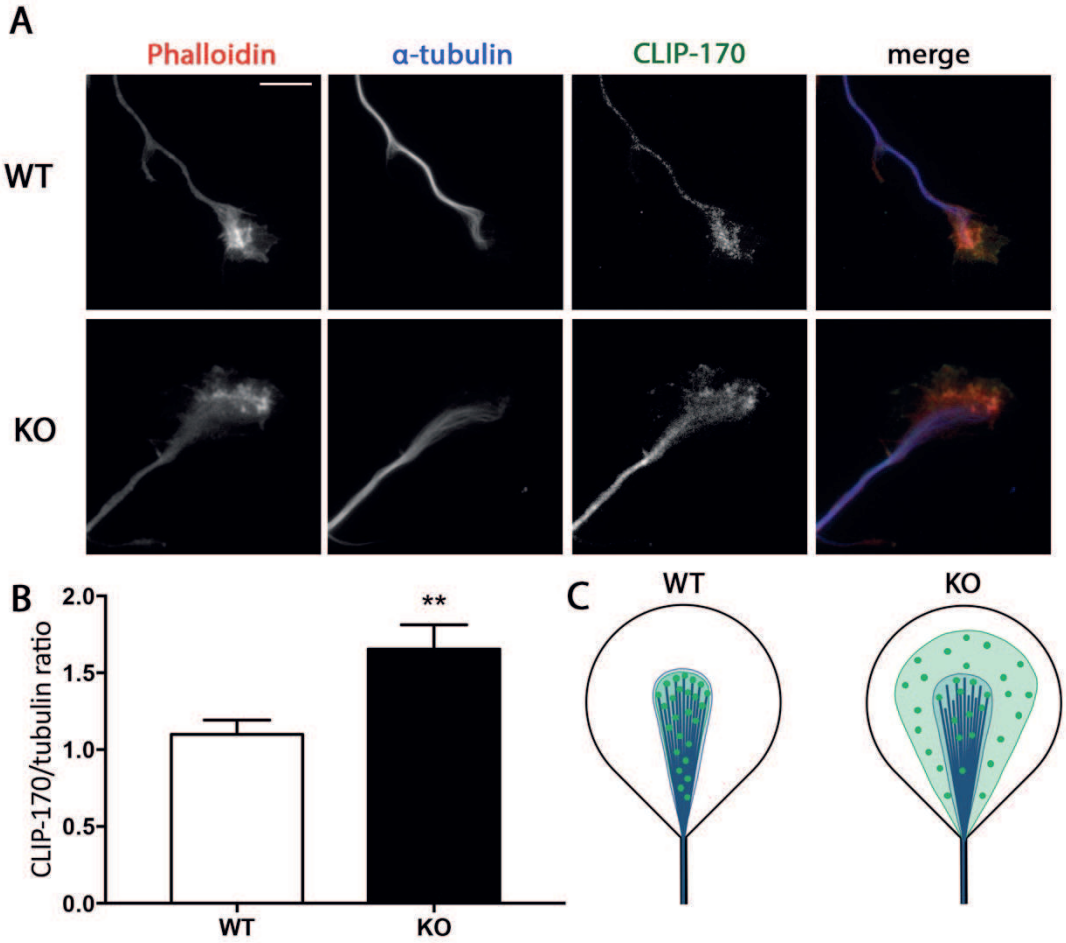

Fig. 4.3 The localization of CLIP-170 on MTs is altered in the absence of Cdkl5. (A) Representative images of WT and *Cdkl5*-KO hippocampal neurons (DIV3) stained for phalloidin (red), -tubulin (blue) and CLIP-170 (green) to visualize actin, MTs and CLIP-170, respectively (scale bar, 10 m). (B) Graph showing the mean CLIP-170/-tubulin ratio in growth cones quantified as described in Materials and methods. (C) Model representing the distribution of CLIP-170 (green dots) and -tubulin (blue filaments) in WT and *Cdkl5*-KO growth cones. In *Cdkl5*-null neurons the area occupied by CLIP-170 (light green) with respect to -tubulin (light blue) is larger than in WT neurons. Data information: data in B are presented as mean SEM (P0.01), Student's t-test. At least 40 neurons for each genotype were analysed from at least three independent experiments.

4.4 CDKL5 is necessary for proper neuronal polarization and extension

Altogether, the above results demonstrate that the loss of CDKL5 alters cell morphology, MT organization, and CLIP-170 dynamicity in COS7 cells. Considering this and our previous publications showing that primary hippocampal neurons silenced for Cdkl5 are characterized by a defect in axon formation and outgrowth [Appendix 1, (*13*, *14*)], we proceeded investigating whether an analogous effect might be present in primary *Cdkl5*-KO hippocampal neurons. We therefore stained DIV4 *Cdkl5*-WT and KO neurons with antibodies against the axonal and dendritic markers, Tau1 and MAP2,

respectively. Correctly polarized neurons were recognized as bearing a single axon with a strong distal staining for Tau1 and several minor MAP2 positive neurites, whereas neurons with no axon or multiple axons were classified as non-polarized. As expected, axon specification occurred in the vast majority of WT neurons, while the loss of Cdkl5 reduced significantly the number of polarized neurons (Fig 4.4 B; WT: 91.88%□0.47; KO: 81.24%□0.66). Moreover, in line with published results obtained in Cdkl5 silenced neurons (*13*), the axon length was significantly reduced in *Cdkl5*□null neurons with respect to the control (Fig 4.4 C; WT: 286.2□m□9.13; KO: 222.9□m□6.03).

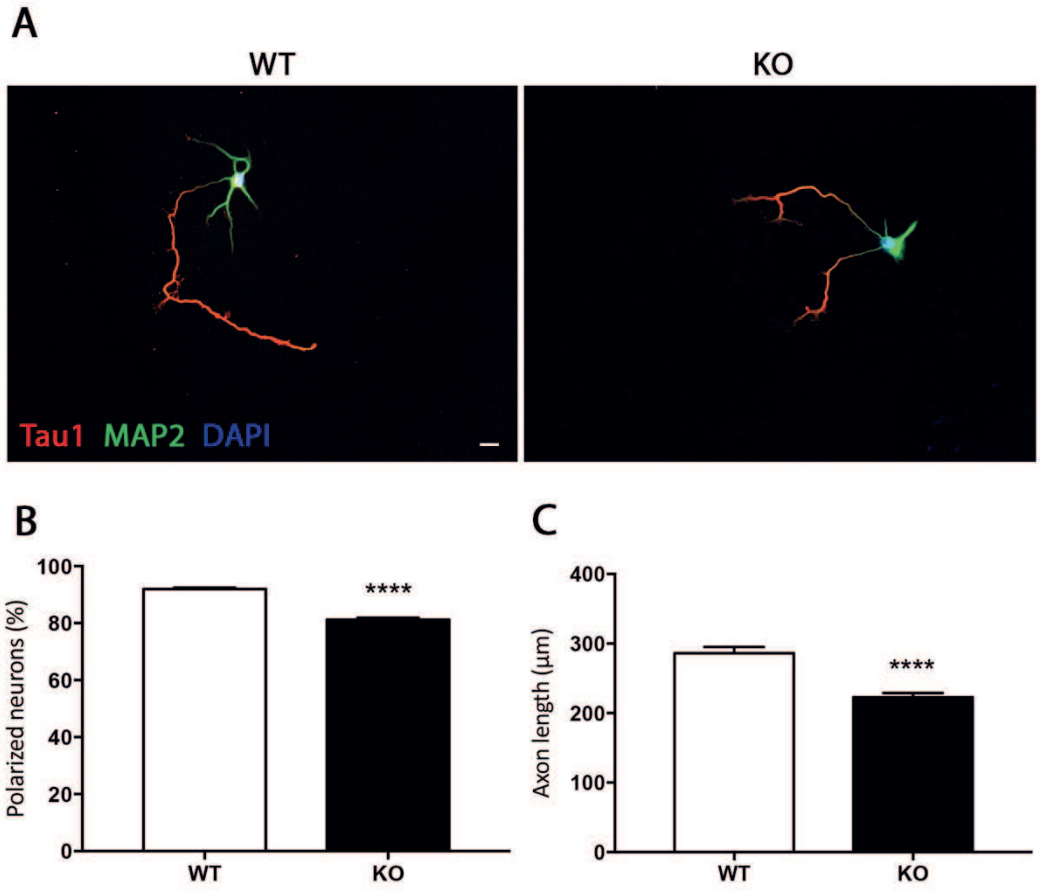

Fig. 4.4 Axon length and polarization are impaired in *Cdkl5*-null neurons. (A) Representative images of WT and *Cdkl5*-KO hippocampal neurons (DIV4) stained for Tau1 (red) and MAP2 (green) to visualize axons and dendrites, respectively. Nuclei were stained with DAPI (blue). Scale bar, 20 □m. (B, C) Graphs showing the mean percentage of polarized neurons and the mean length of axons in WT and *Cdkl5*-KO neurons. Data information: data in B and C are presented as mean □SEM (□□□□ P□0.0001). Student's t-test. At least 300 or 180 neurons, for polarization or elongation, respectively, were analysed for each genotype in five independent neuronal preparations.

4.5 CLIP-170 is present in dendritic spines of primary hippocampal neurons

Dendritic spines are tiny protrusions that serve as a platform for post-synaptic specializations as exemplified by the clustering of neurotransmitter receptors at the post-synaptic density (PSD). The actin cytoskeleton has for years been considered the major cytoskeletal structure that controls and regulates spine formation and dynamics (*107*). Only in the last years, the presence of MTs and the associated proteins has been demonstrated in spines and their role in spine plasticity has become the object of several studies. Indeed, MTs guided by plus end tracking proteins (+TIPs), such as EB3, have been found to enter dendritic spines in a transient and dynamic manner. The high dynamicity with which this occurs seems to be fundamental for spine formation and maintenance (*108*).

Dendritic spines, similar to the growth cone, represent a highly active area where MT dynamicity contributes to cellular plasticity (*20*). We speculate that impaired CLIP-170 functioning might contribute to the spine defects in *Cdkl5*-null neurons by reducing the spine invasion of MTs. Albeit it has been noted that the mutation of an ortholog of CLIP-170, CLIP1, cause intellectual disability (*109*), its localization in the post-synaptic compartment has never been reported. To address this, neuronal cultures were prepared from WT mouse embryos at E18 and transfected with a GFP-expressing vector at DIV11 and harvested at DIV15 when neurons under our culture conditions have reached the mature state. This approach allowed us to visualize neuronal architecture including dendritic spines and therefore to allocate the distribution of CLIP-170. As shown in figure 4.5 A, CLIP-170 could be easily be detected in dendritic spines. This evidence was further confirmed through the biochemical fractionation of hippocampal neurons into synaptosomes that are enriched in pre- and post-synaptic proteins such as PSD95 (Fig. 4.5 B). In line with the IF assay, CLIP-170 can be detected in synaptosomal (Syn) fractions. Interestingly, synaptosomes of *Cdkl5*-KO neurons presented a significant reduction of CLIP-170 whereas no difference could be observed in the amount of GAPDH (Fig. 4.5 B and C. Fold change expression KO/WT: CLIP-170: 0.47±0.08; GAPDH: 1.14±0.1). Of note, total levels of CLIP-170 were negatively influenced by loss of Cdkl5 (Fig. 4.5 D. Fold change expression KO/WT: KO: 0.55±0.06) but since we found that the

ratio of Syn/Input CLIP-170 is reduced (Fig. 4.5 E), we envisage that loss of Cdkl5 affects both CLIP-170 expression and synaptic localization.

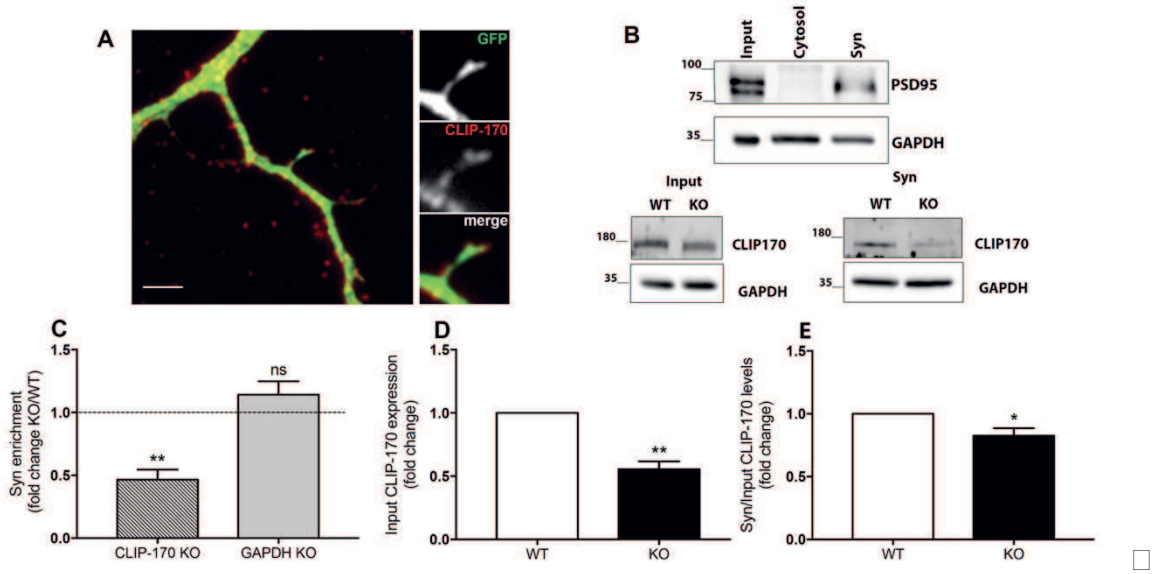

Fig. 4.5 CLIP-170 localizes in dendritic spines. (A) Representative image of DIV15 WT hippocampal neurons stained for GFP and CLIP-170 to visualize spines and CLIP-170 localization, respectively. Scale bar, 5 ⍰m. (B) Representative WBs showing the level of the synaptic protein PSD95 in total lysate (Input) before fractionation and in the cytosolic (cytosol) and synaptosomal (Syn) fractions after fractionation. The lower WBs show levels of CLIP-170 (and GAPDH as internal standard) in total lysates (Input) and synaptosomal fraction (Syn) of WT and *Cdkl5*-KO hippocampal lysates. (C) Graph showing the ratio of CLIP-170 and, as control, GAPDH levels (fold change) in synaptosomal fractions of *Cdkl5*-KO neurons compared to WT controls (dotted line). (D) Graph showing CLIP-170 expression levels (fold change) in *Cdkl5*-KO hippocampal lysates compared to the WT counterpart before fractionation. (E) Graph showing Syn/Input ratio of CLIP-170 expression in WT and *Cdkl5*-KO hippocampal lysates. Data information: data in C, D and E are presented as as mean ⍰SEM (⍰⍰ P⍰0.01, ⍰ P⍰0.05). Student's t-test. Three independent synaptosomal fractionations were analysed from three different animals (PND60) for each genotype.

4.6 The loss of Cdkl5 results in reduced spine density and maturation in cultured hippocampal neurons

In hippocampal neurons, Cdkl5 is present both in the nucleus and in the cytoplasm where it can be detected along the dendrites and at the level of dendritic spines. Importantly, the silencing of Cdkl5 results in impaired synaptic connections and spine structures (*9*). Primary cultures of hippocampal neurons constitute a well-accepted in vitro experimental system that undergoes differentiation and maturation, reproducing some critical steps of in vivo development, including synaptogenesis. To evaluate how the loss of Cdkl5 influences spine density under these conditions we took advantage of WT and *Cdkl5*-KO primary hippocampal neurons transfected with a GFP-expressing

vector at DIV11 and harvested at DIV15. As shown in figure 4.6, we registered a reduction in spine density in *Cdkl5*-KO neurons compared to the WT controls (Fig. 4.6 A. Number of protrusions: WT:10.95±0.59; KO: 8.36±0.67). Dendritic spines are heterogeneous in size and shape and can be classified as immature (filopodia, thin-shaped) and mature spines (mushroom- and cup-shaped) (Fig. 4.6 B). Interestingly, analysing the morphology of the dendritic spines of *Cdkl5*-KO hippocampal neurons we observed a lower percentage of mature spines than in WT neurons, accompanied by an increased percentage of immature spines (Fig. 4.6 C and D. Mature WT: 34.49%±2.62; Immature WT: 65.51%±2.58; Mature KO: 22.92%±2.69; Immature KO: 77.08%±2.45). These data recapitulate previously published results indicating that Cdkl5 is required to ensure correct spine maturation. Moreover, in line with literature describing that the presence of PSD95 in the glutamatergic dendritic spine is an indicator of its maturation (*110*), PSD95 levels are reduced in the absence of Cdkl5. To understand whether a similar defect could be detected in our cultures of primary neurons, we performed immunocytochemistry experiments in which neurons were stained with antibodies against PSD95 and the dendritic marker MAP2. As shown in the representative immunofluorescence (Fig. 4.6 E), the number of PSD95 immunoreactive *puncta* in dendrite segments from *Cdkl5*-KO hippocampal neurons were visibly reduced compared to the WT counterpart. The quantification confirmed this evidence, showing that loss of Cdkl5 causes a significant and robust loss of excitatory post-synaptic contacts (Fig. 4.6 F. Number of *puncta*: WT: 11.82±0.49; KO: 8.7±0.4).

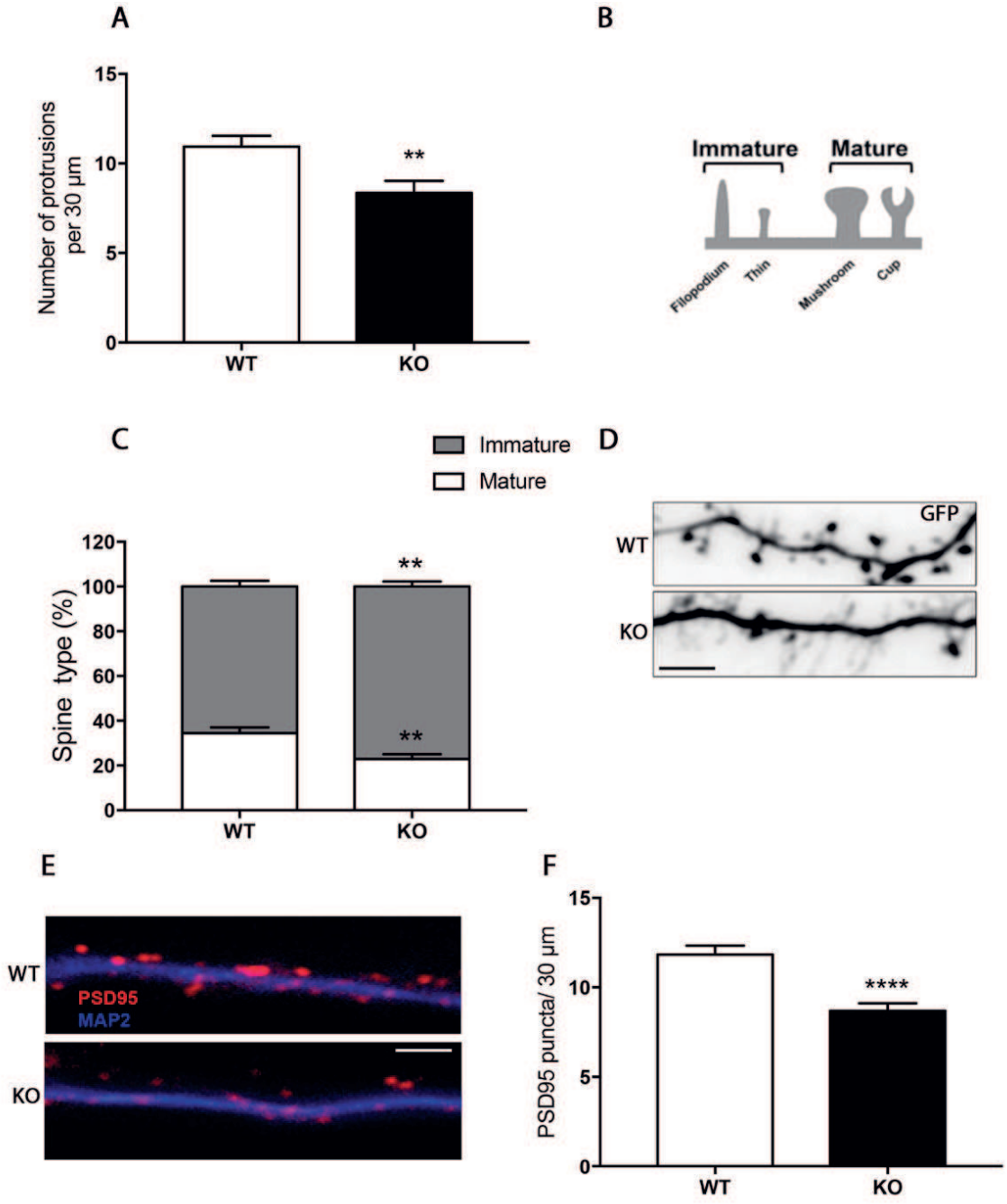

Fig. 4.6 Spine density and maturation are altered in *Cdkl5*-KO neurons. (A) Graph showing the mean number of spine protrusions of 30 µm long dendritic segments of cultured WT and *Cdkl5*-KO hippocampal neurons (DIV15). (B) Diagram showing immature spines (filopodium-like and thin-shaped) and mature spines (mushroom- and cup-shaped) (adapted from (*7*)). (C) Graph showing the mean percentage of mature and immature spines in relation to the total number of protrusions in WT and *Cdkl5*-KO neurons. (D) Representative images of dendritic branches from GFP-positive *Cdkl5*-WT and KO neurons at DIV15. Neurons in A-D were transfected with a GFP-expressing vector at DIV11 and analysed at DIV15. Scale bar: 5 µm. (E) Representative images of WT and *Cdkl5*-KO hippocampal neurons (DIV15) stained with antibodies against the post-synaptic density protein 95 (PSD95; red) and MAP2 (blue) to visualize mature spines and neuronal dendrites, respectively. Scale bar: 5 µm. (F) Graph showing the mean number of PSD95 *puncta* of 30 µm long dendritic segments from cultured WT and *Cdkl5*-KO hippocampal neurons. Data information: data in A, C and F are presented as mean ±SEM (** P≤0.01; **** P≤0.0001). At least 30 dendritic segments were analysed for spine density, type or PSD95 *puncta* for each genotype in five independent neuronal preparations. A and F: Student's t-test. C: Two-way-ANOVA followed by Sidak's post hoc analysis.

4.7 Pregnenolone and PME induce the open conformation of YFP–CLIP-170–CFP in CDKL5-deficient cells

As mentioned above, the activity of CLIP-170 is tightly regulated by its specific conformation: when opened, CLIP-170 can interact with MTs and its COOH-terminal partners, while its folded conformation blocks its association with other proteins (*19*).

CLIP-170 has recently been identified as a cellular receptor for the neurosteroid Pregnenolone. By binding CLIP-170, P5 stabilizes the extended conformation of the protein thus increasing its affinity for MTs and promoting MT polymerization (*21*). P5 is synthesized from cholesterol by CYP11A1 and can be further metabolized into other steroids that can accomplish different functions, including the interaction with membrane bound receptors and the regulation of gene expression. The above data suggest that CLIP-170 is mainly in a closed inactive conformation in the absence of CDKL5. We thus hypothesized that P5 might be capable of enhancing the open conformation of CLIP-170, correcting some of the cellular defects associated with CDKL5 deficiency. To be able to attribute any effect to P5, we alongside used PME, a non-metabolizable synthetic derivative of P5, which promotes MT dynamics like P5 (*111*), but is devoid of the downstream effects possibly linked to the further metabolism of P5 (*112*).

We thus treated siCDKL5-COS7 cells expressing YFP–CLIP-170–CFP with P5 or PME and examined by FRET analysis the intramolecular state of CLIP-170 by live microscopy acquisition. Intriguingly, our preliminary data showed that chronic treatment of siCDKL5 cells with P5 or PME reduced the YFP–CLIP170–CFP FRET efficiency. Such reduction is compatible with the specific capacity of the two compounds to target CLIP-170, stabilizing its open active conformation. Indeed, the treatment with P5 significantly reduced FRET efficiency from 73.21%±3.77 of siCDKL5 NT cells to 54.34%±3.37 (Fig. 4.7 A). Similarly, PME showed a clear tendency in the same direction of P5, producing a reduction of FRET efficiency to 55.51%±4.51 (P value≈0.08. Statistical analysis in figure 4.7 B).

Altogether, these data confirm previous publications that demonstrated a specific action of P5 on CLIP-170, promoting a conformational change of the protein from a folded inactive to an open active state (*113*). Remarkably, considering that the activity

of PME has so far been restricted to the regulation of tubulin assembly via MAP2 (*22*, *111*), our data uncover a novel target of this compound.

A

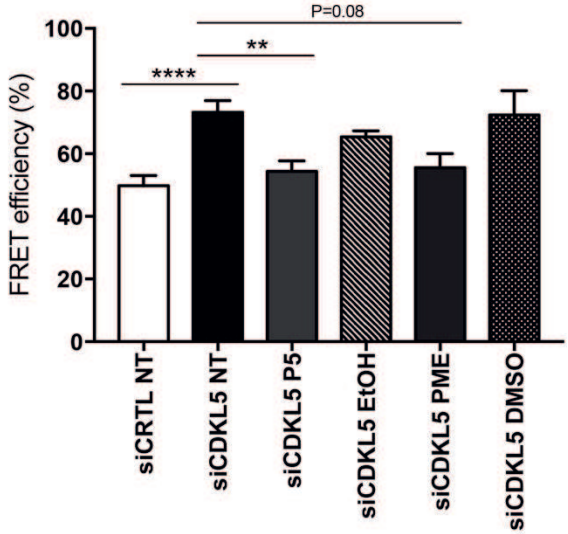

B

Sample A		Sample B	Mean ± SEM A	Mean ± SEM B	P value
siCTRL NT	vs	siCDKL5 NT	49.8%±3.29	73.21%±3.77	<0,0001
siCTRL NT	vs	siCDKL5 P5	49.8%±3.29	54.34%±3.37	0,9429
siCTRL NT	vs	siCDKL5 EtOH	49.8%±3.29	65.36%±4.51	0,0114
siCTRL NT	vs	siCDKL5 PME	49.8%±3.29	55.51%±4.51	0,9511
siCTRL NT	vs	siCDKL5 DMSO	49.8%±3.29	72.28%±7.74	0,0029
siCDKL5 NT	vs	siCDKL5 P5	73.21%±3.77	54.34%±3.37	0,0038
siCDKL5 NT	vs	siCDKL5 EtOH	73.21%±3.77	65.36%±4.51	0,5445
siCDKL5 NT	vs	siCDKL5 PME	73.21%±3.77	55.51%±4.51	0,0825
siCDKL5 NT	vs	siCDKL5 DMSO	73.21%±3.77	72.28%±7.74	>0,9999
siCDKL5 P5	vs	siCDKL5 EtOH	54.34%±3.37	65.36%±4.51	0,2473
siCDKL5 PME	vs	siCDKL5 DMSO	55.51%±4.51	72.28%±7.74	0,2315

Fig. 4.7 P5 and PME stabilize the extended conformation of CLIP-170. (A) Graph showing the mean percentage of FRET efficiency in CDKL5 silenced cells (siCDKL5) compared to control cells (siCTRL). Cells were left untreated or treated daily with 1 ?M P5 or PME, or the respective vehicles (0.0032% EtOH and 0.001% DMSO). Data information: data are shown as mean?SEM (???? P?0.0001; ?? P?0.01), ANOVA followed by Tukey's post hoc analysis. At least 25 cells for each condition were analysed from three independent experiments. For siCDKL5 PME/DMSO 10 cells were analysed in one experiment. (B) Table showing the statistical analysis of data presented in A.

4.8 PME enhances the binding of GFP–CLIP-170 to MTs in CDKL5-deficient cells

Exploiting time-lapse microscopy of a GFP-tagged CLIP-170 construct, we recently demonstrated that P5 is capable of enhancing the binding of GFP–CLIP-170 to MTs in COS7 cells depleted of CDKL5. Indeed, CLIP-170 accumulates at the plus-end of growing MTs forming comet-like structures: the loss of fluorescence in the comet-like dashes is correlated with the dissociation of CLIP-170 from MTs (*114*). By increasing the affinity of CLIP-170 for MTs, P5 promotes their dynamicity, which results in an increased length and duration of GFP–CLIP-170 comets. Considering the above results on FRET efficiency, indicating that PME could exert a role on the conformational state of CLIP-170, we hypothesized that this synthetic P5 derivative might be capable, like P5, of rescuing the defective MT-binding of CLIP-170 in CDKL5 depleted cells [Appendix 1, (*14*)]. To test this, we treated siCDKL5-COS7 cells expressing GFP–CLIP-170 with 1 M PME and analysed the fluorescent comets through time-lapse microscopy. Intriguingly, we found that chronic treatment of siCDKL5 cells with PME produced an increase in the length (Fig. 4.8 B. siCTRL: 4.35 m 0.28; siCDKL5 DMSO: 2.36 m 0.16; siCDKL5 PME: 3.3 m 0.23) and duration (Fig. 4.8 C. siCTRL: 30.01 sec 1.72; siCDKL5 DMSO: 14.67 sec 1.24; siCDKL5 PME: 23.38 sec 1.6) of GFP–CLIP-170 positive comets in treated cells with respect to the control cells.

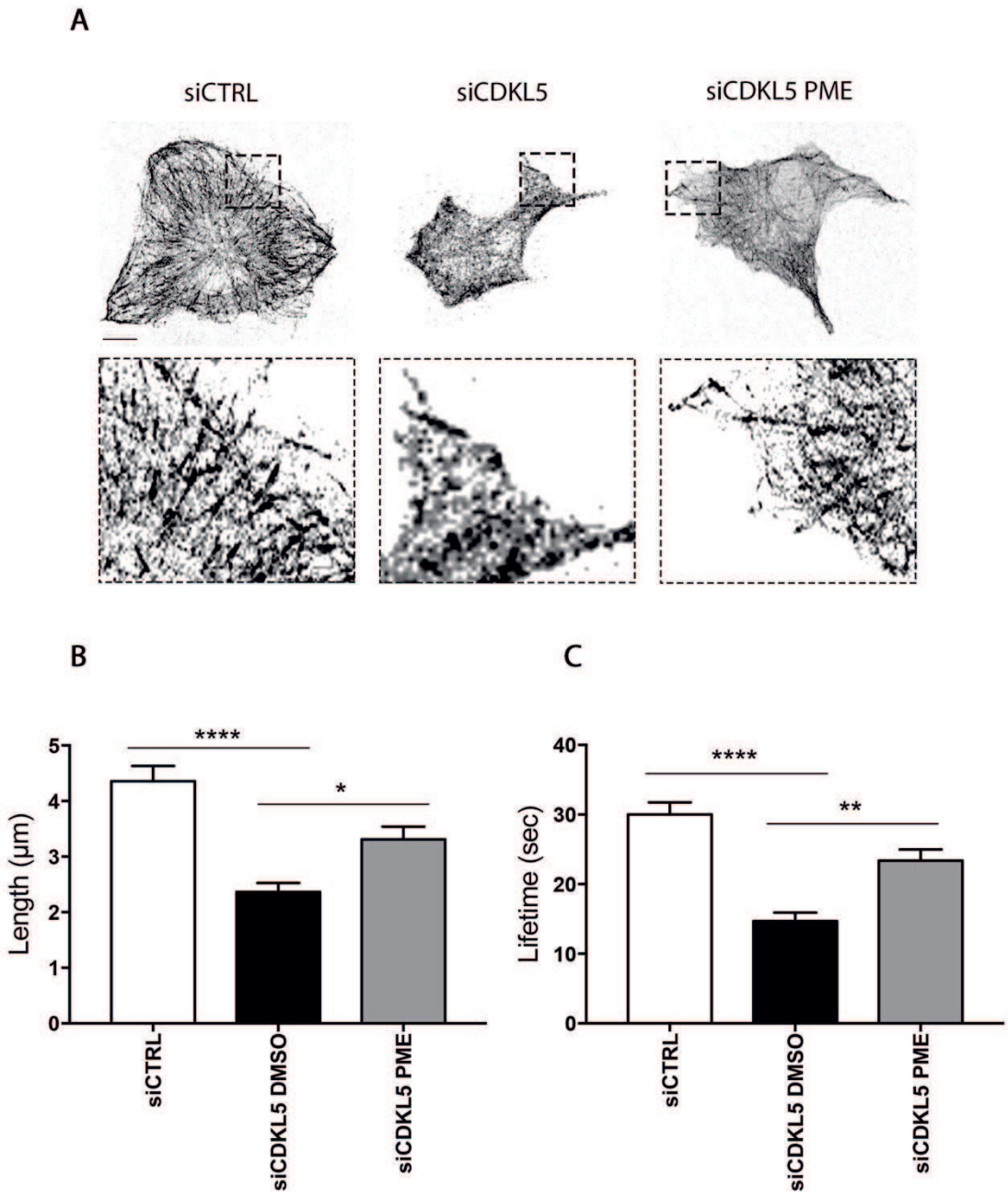

Fig. 4.8 PME ameliorates the dynamics of CLIP-170 on MTs. (A) Representative images of GFP-CLIP-170 expressing COS7 cells silenced and treated with 1 ?M PME or vehicle (0.001% DMSO) for 72 h. Boxed areas are magnified underneath. Scale bar: 10 ?m. (B, C) Graphs showing the mean length and lifetime of GFP–CLIP-170 comets in COS7 cells silenced for CDKL5 or with a control siRNA and treated as in A. Data information: data are presented as mean ?SEM (????P?0.0001; ?? P?0.01; ?P?0.05), ANOVA followed by Tukey's post hoc analysis. At least 15 comets for each condition were analysed from at least three independent cells.

4.9 Cdkl5-related growth cone defects are ameliorated by P5 and PME treatments

Cytoskeletal dynamics play a key role during the first steps of neuronal development (*115*) and, in particular, +TIPs, such as CLIP-170 (*16*), enable neuronal polarization by enhancing the stability of MTs in the axon. Our results indicate that the loss of CDKL5 negatively impacts CLIP-170 dynamics on MTs, probably producing alterations in cell morphology. Encouraged by the positive effect of P5 and PME on the conformational state of CLIP-170, we found it interesting to analyse the capacity of the two compounds to restore axonal defects linked to Cdkl5 in young neurons. For this purpose we analysed different growth cone phenotypes in WT and *Cdkl5*-KO neurons at DIV3 upon treatment for 48 hours with P5 or PME (both 1 μM) or the respective vehicles (P5: 0.0032% EtOH; PME: 0.001% DMSO). Progesterone (P4; 1 μM), a metabolite of P5 devoid of any effect on CLIP-170 (*21*), was used as internal negative control. We first considered growth cone morphology. As shown in figure 4.9 A, both compounds displayed a significant effect on growth cone morphology. Indeed, P5 reduced the area occupied by MTs at the tip of the axon from 67.53 μm2 5.52 in vehicle (EtOH) treated *Cdkl5*-KO neurons to 38.92 μm2 2.28. A similar effect was observed with PME (WT NT: 41.75 μm^2 2.15; KO NT: 71.26 μm^2 1.91; KO DMSO: 65.24 μm^2 3.65; KO PME: 37.31 μm^2 2.38). Contrariwise, no effect was observed in P4 treated neurons (Fig. 4.9 B, left. KO P4: 65.2 μm^2 4.93). Considering that an enlargement of the growth cone area is often associated with a paused state with MTs forming loops, we proceeded analysing the effect of P5 and PME on the paused phenotype described above in *Cdkl5*-KO neurons. We found that both compounds resulted in a reduced number of paused growth cones. Indeed, P5 displayed a trend in decreasing such phenotype in *Cdkl5*-KO neurons with respect to *Cdkl5*-KO vehicle treated neurons (KO P5 13.7% 2.6; KO EtOH: 36.0% 7.48). Similarly, just 12.3% 4.83 of PME-treated *Cdkl5*-KO neurons displayed a paused phenotype (KO DMSO: 40.0% 5.77). Neither vehicles nor P4 produced any effect on such alteration (Fig. 4.9 C. KO NT: 37.3% 6.36; KO P4: 40.0% 8.16). Lastly, we analysed the localization of CLIP-170 at the growth cone level upon treatment with P5 and PME. Our results indicate that both compounds influenced the distribution of CLIP-170 at the tip of the axon, increasing its co-localization with tubulin (Fig. 4.9 D, left):

indeed, the CLIP-170/□TUB ratio decreased from 1.71□0.21 and 1.51□0.3 in vehicle treated *Cdkl5*□KO control neurons (EtOH and DMSO respectively) to 1□0.26 in P5-treated and to 1.07□0.2 in PME-treated *Cdkl5*-null neurons. No effects were observed in neurons treated with vehicles (WT NT: 1.1□0.; 1 KO NT: 1.65□0.16). Importantly, in *Cdkl5*-WT neurons neither of the compounds affected the growth cone area (Fig. 4.9 B, right. WT P5: 35.79 □m^2□2.59; WT EtOH: 43.16□m^2□4.31; WT PME: 40.29□m^2□4.14; WT DMSO: 44.17□m^2□5; WT P4: 46.92□m^2□5.6), the paused state (Fig. 4.9 C, right. WT P5: 2.5%□2.5; WT EtOH: 14.8%□3.02; WT PME: 9.6%□44.1; WT DMSO: 15%□6.45; WT P4: 22.5□4.79) and CLIP-170 localization (Fig. 4.9 D, right. CLIP-170/□TUB ratio: WT P5: 1.13□0.13; WT EtOH: 1.06□0.1; WT PME: 1.09□0.19; WT DMSO: 1.1□0.12). These results, even if preliminary, indicate a positive effect of both P5 and PME on growth cone defects associated with the loss of Cdkl5.

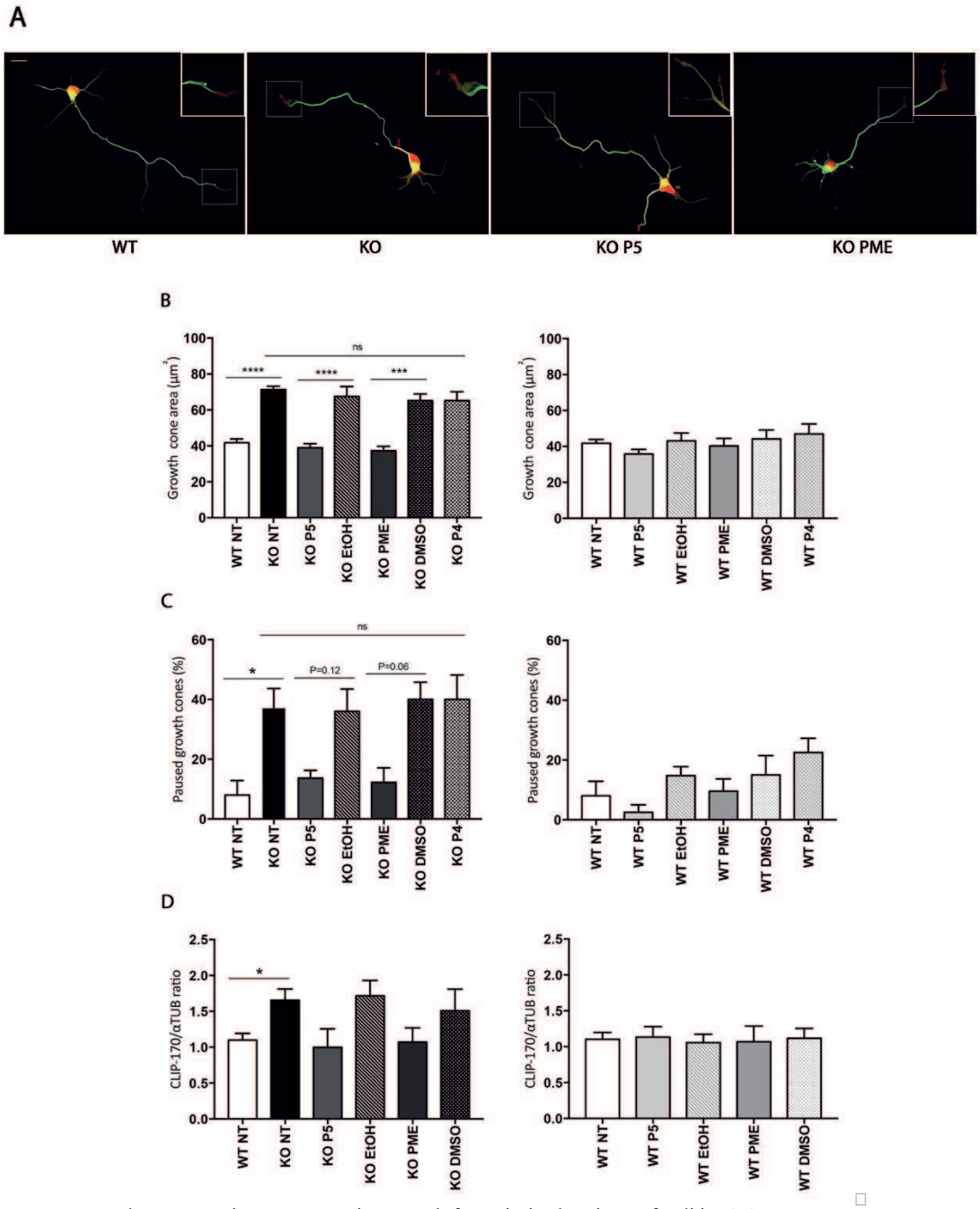

Fig. 4.9 P5 and PME ameliorate growth cone defects linked to loss of Cdkl5. (A) Representative images of WT and *Cdkl5*KO hippocampal neurons (DIV3) stained for -tubulin (green) and phalloidin (red) to visualize microtubules and actin, respectively. (B) Graphs showing the mean microtubule area in WT and *Cdkl5*-KO growth cones treated with 1 M P5, PME, P4 or vehicles (0.0032% EtOH and 0.001% DMSO) and quantified as described in Materials and methods. Data information: data in B are presented as mean SEM (P0.0001), ANOVA followed by Tukey's post hoc analysis. At least 40 neurons were analysed for each condition in three independent neuronal preparations. (C) Graphs showing the mean percentage of WT and *Cdkl5*-KO paused growth cones treated as described in B. Data information: data in C are presented as mean SEM (P0.01; P0.05), ANOVA followed by Tukey's post hoc analysis. At least 40 neurons were analysed for each condition in three independent neuronal preparations. (D) Graphs showing the mean CLIP-170/tubulin ratio in WT and *Cdkl5*-KO growth cones treated with 1 M P5, PME and vehicles (0.0032% EtOH and 0.001% DMSO). Data information: data in D are presented as mean SEM (P0.05), ANOVA followed by Tukey's post hoc analysis. At least 10 neurons were analysed for each condition in three independent neuronal preparations.

4.10 P5 and PME normalize axon length and polarization in *Cdkl5*-KO neurons

In light of the above data, we speculated that the beneficial effects of P5 and PME on Cdkl5-dependent growth cone defects could have a positive repercussion on the defective axon formation and outgrowth in *Cdkl5*-null neurons. We thus treated *Cdkl5*-WT and KO primary hippocampal neurons for 72 h with P5 or PME (or the respective vehicles EtOH and DMSO) before fixation at DIV4 and stained the neurons for the axonal and dendritic markers, Tau1 and MAP2, respectively (Fig. 4.10 A). Parallel experiments were performed with P4. Correctly polarized neurons were recognized, as previously described, as those bearing a single axon with a strong distal staining for Tau1, whereas neurons with no axon or multiple axons were classified as non-polarized (Fig. 4.10 B). Interestingly, the treatment with P5 or PME for three days was sufficient to completely correct axon specification. Indeed, the number of polarized neurons was similar to that of WT neurons (WT NT: 91.98%±0.47; KO NT: 81.24%±0.66; KO P5: 92.12%±0.7; KO EtOH: 81.75%±2.39; KO PME: 90.67%±1.83; KO DMSO: 81.21%±3.55). As before, P4 was incapable of restoring the axonal defects linked to the loss of Cdkl5 (KO P4: 81.41%±3.76). Similarly, both P5 and PME but not P4 were capable of normalizing axon length (Fig. 4.10 C; WT NT: 286.2±m± 9.13; KO NT: 222.9±m±6.03, KO P5: 320.2±m±18.56; KO EtOH: 210.9±m±11.58; KO PME: 321.9±m±18.23; KO DMSO: 228.7±m±0.95; KO P4: 248.5±m±1.86). Neither of the compounds affected polarization or axon length in *Cdkl5*-WT neurons (Fig. 4.10 B and C; polarization, WT NT: 91.98%±0.47; WT P5: 92.2%±1.86; WT EtOH: 89.77%±1.29; WT PME: 91.29%±0.71; WT DMSO: 90.53%±1.3; WT P4: 93.15%±3.15; axon length, WT NT: 286.2±m±9.13; WT P5: 312.2±m±6.56; WT EtOH: 289.2±m±16.41; WT PME: 299.8±m±14.63; WT DMSO: 276.6±m±18.14; WT P4: 314.4±m±5.8). Altogether, P5 and PME are capable of causing a robust rescue of various defects linked to Cdk5 in young neurons.

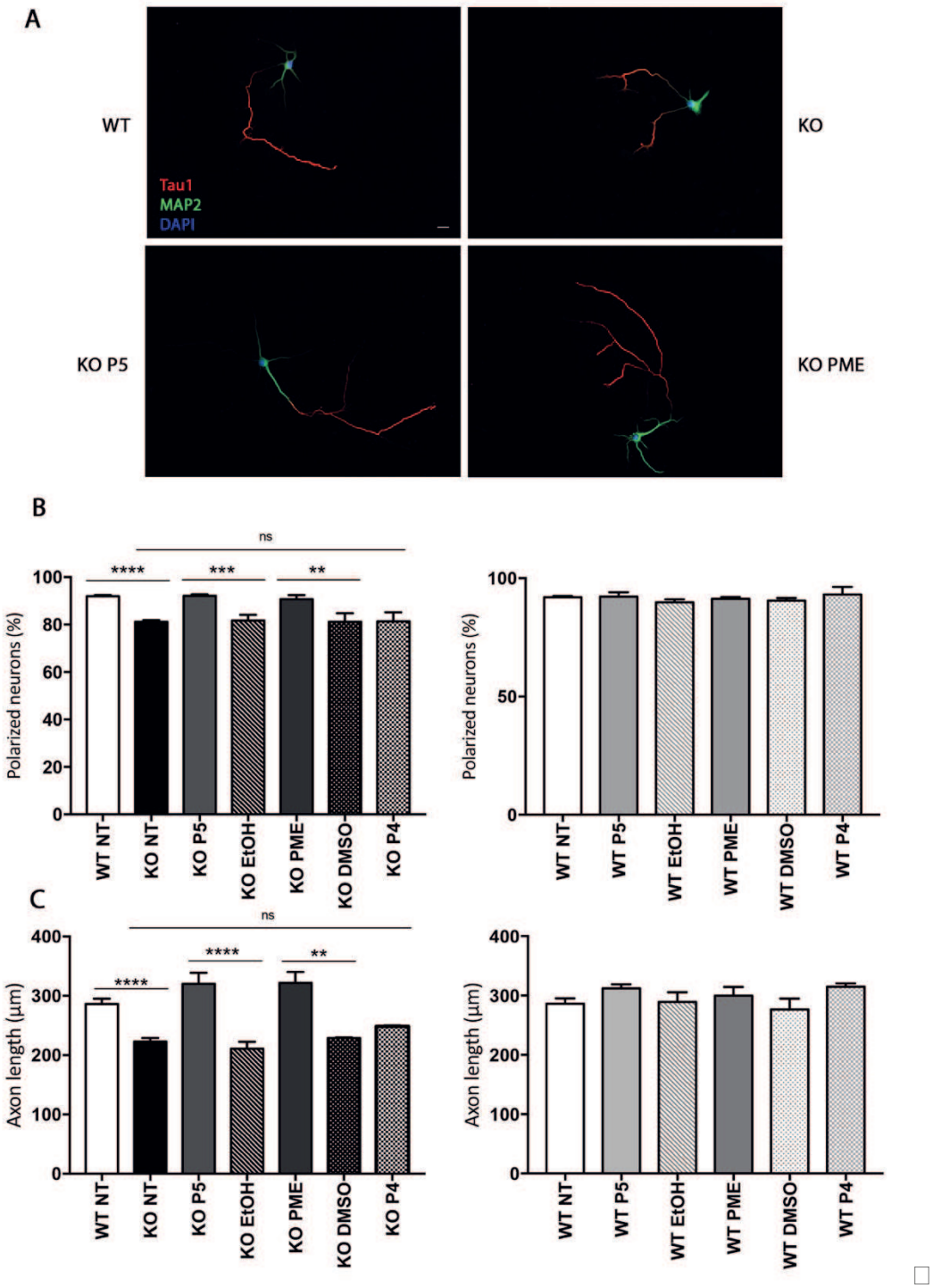

Fig. 4.10 P5 and PME correct axonal impairment caused by the loss of Cdkl5. (A) Representative images of WT and *Cdkl5*-KO hippocampal neurons (DIV4) stained for Tau1 (red) and MAP2 (green) to visualize axons and dendrites, respectively. Nuclei were stained with DAPI (blue). Neurons were left untreated or were treated with 1 ?M P5 or PME for 72 h. EtOH (0.0032%) was used as vehicle for P5 and DMSO (0.001%) for PME. Scale bar: 20 ?m. (B) Graphs showing the mean percentage of polarized primary hippocampal neurons. Both *Cdkl5*?WT and KO neurons were left untreated or were treated as in A using P4 (1?M) as negative control. (C) Graphs showing the mean length of axons in primary hippocampal neurons. *Cdkl5*-WT and KO neurons were left untreated or treated as in B. Data information: data in B and C are presented as mean ?SEM (???? P?0.0001; ???P?0.001;), ANOVA followed by Tukey's post hoc analysis. At least 120 or 60 neurons, for polarization or elongation, respectively, were analysed for each condition in three independent neuronal preparations.

4.11 P5 and PME treatments restore synaptic maturation in *Cdkl5*-null neurons

Intrigued by the above results, we speculated that P5 and PME might be capable of rescuing not only axonal phenotypes in young neurons, but also the dendritic spine defects associated with loss of Cdkl5.

To evaluate the effect of both compounds, neuronal cultures were prepared from WT and *Cdkl5*-KO mouse embryos and transfected with a GFP-expressing vector at DIV11 to visualize neuronal morphology and harvested at DIV15. Neurons were left untreated or treated for four days with 1 M P5, PME or the respective vehicles (0.0032% EtOH, 0.001% DMSO) at DIV11. Remarkably, our results indicate that P5 or PME exerted an effect on the morphology of dendritic spines of *Cdkl5*-KO neurons producing a clear tendency in increasing the number of mature spines compared to vehicle-treated neurons (Fig. 4.11 A. Mature WT: 34.49%2.62; Immature WT: 65.51%2.59; Mature KO: 22.82%2.2; Immature KO: 77.08%2.45; Mature KO P5: 41.07%10.13; Immature KO P5: 58.84%10.14; Mature KO EtOH: 22.4%6.74; Immature KO EtOH: 77.23%6.82; Mature KO PME: 32.4%11.73; Immature KO PME: 67.56%11.72; Mature KO DMSO: 22.12%2.92; Immature KO DMSO: 74.84%2.93).

Moreover, to evaluate further the effect of the two compounds in restoring spine maturation we also considered the number of PSD95 clusters (Fig. 4.11 C). Expectedly, both compounds proved capable of rescuing also this parameter. Indeed, the number of PSD95 *puncta* in 30 m long dendritic segments of P5 and PME treated KO neurons was similar to that of the WT control neurons (Fig. 4.11 B. WT NT: 11.820.49; KO NT: 8.70.4; KO P5: 11.080.52; KO EtOH: 8.850.52; KO PME: 10.590.46; KO DMSO: 8.720.44).

Altogether, these data show that P5 and PME are both capable of rescuing neuronal defects linked to Cdkl5 both in young and in mature primary hippocampal neurons.

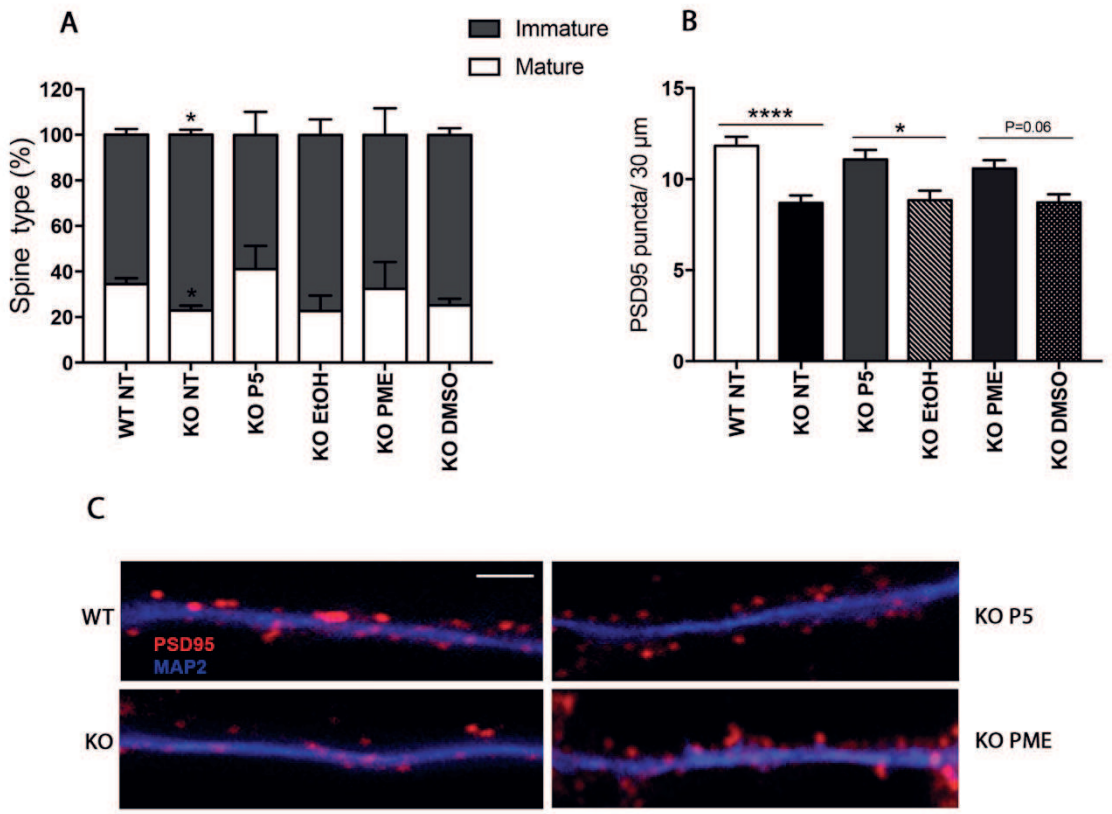

Fig. 4.11 P5 and PME revert defective dendritic spine maturation in Cdkl5 deficient neurons. (A) Graph showing the mean percentage of mature and immature spines in relation to the total number of protrusions in WT and *Cdkl5*-KO neurons. Neurons were left untreated or treated with 1 µM P5 and PME or the respective vehicles (0.0032% EtOH and 0.001% DMSO). Data information: data in C are presented as mean ±SEM (* P<0.05), Two-way ANOVA followed by Sidak's post hoc analysis. At least 30 dendritic segments for spine type were analysed for each condition in five independent neuronal preparations. (B) Graph showing the mean number of PSD95 *puncta* of 30 µm long dendritic segments from neurons treated as in A. Data information: data in B are presented as mean ±SEM (**** P<0.0001; *P<0.05), ANOVA followed by Tukey's post hoc analysis. At least 40 dendritic segments were analysed for each genotype in three independent neuronal preparations. (C) Representative images showing PSD95 staining in dendritic segments of WT and *Cdkl5*-KO neurons fixed at DIV15. Neurons were left untreated or treated as in A. Neurons were stained with the dendritic marker MAP2 (blue) and the mature spine marker PSD95 (red). Scale bar: 5 µm.

5. Discussion

CDKL5 disorder is a severe neurodevelopmental disease caused by mutations in the homonymous gene, located on the X chromosome (*35*). Due to the presence of several features overlapping with classic Rett syndrome, CD was initially categorized as a RTT variant (*36*) but is now considered an independent clinical entity (*2*). A full clinical picture of CD is still limited as a broader number of patients is needed to delineate more thoroughly the natural history of this disease and to identify its main features. However, CD is characterized, in the majority of cases, by the onset of intractable convulsive seizures within the first three months after birth, intellectual disability, gross motor impairment, hand apraxia and stereotypies, compromised language skills, and some dysmorphic facial features such as prominent and broad forehead, high hairline and deep-set eye (*2*).

Although there have been important steps towards an increased knowledge of CDKL5 functions since the discovery of its involvement in neurological disorders (*1*), more are still needed to allow the development of therapeutic strategies for CD. CDKL5 is a serine-threonine kinase, which shuttles between the nucleus and the cytoplasm (*49*) where it regulates several cellular processes through its interacting proteins. In the nucleus CDKL5 interacts with MeCP2 (*4*, *44*), DNMT1 (*5*), the splicing factor SC35 (*6*) and HDAC4 (*7*), thus suggesting a link between CDKL5 and gene expression. Cytoplasmic CDKL5 is known to regulate several aspect of neuronal maturation and morphology: indeed, it seems to have a role in the activation and maintenance of synaptic activity (*116*) and in the regulation of neuronal morphogenesis and dendritic arborization in a Rac1-dependent manner (*8*). Proper spine development and synapse stabilization and function were also found to depend on the presence of functional CDKL5 in accordance with its interaction with PSD95, NGL-1 and Amph1 (*9*–*12*). Besides a clear involvement in shaping the dendritic arbour and synaptic spines, CDKL5 has been also shown to take part in the early phases of neuronal development. Indeed, CDKL5 was demonstrated to play a role in the regulation of axon specification and elongation at least in part through its interaction with Shootin1 (*13*).

The strong impact of CDKL5 on neuronal morphology suggests that the kinase may be involved in regulating cytoskeletal dynamics. However, the molecular mechanisms linking CDKL5 to such processes have so far remained obscure. Intriguingly, we recently demonstrated that CDKL5 is able to regulate MT dynamics thanks to its interaction with IQGAP1. Among other functions, IQGAP1 regulates the correct interaction between MTs and actin networks, through the formation of a triple complex with activated Rac1 and the +TIP CLIP-170 (*15*). The absence of CDKL5 causes the deregulation of the Rac1–IQGAP1–CLIP-170 complex, the delocalization of IQGAP1 from the leading edge and the reduction of the affinity of CLIP-170 for the plus end of MTs, leading to impaired cell migration [Appendix 1, (*14*)].

5.1 CDKL5 influences CLIP-170 functionality

The +TIP CLIP-170 regulates MT dynamics by binding specifically to the plus ends of growing MTs, serving as a rescue factor that supports the growth and elongation of MTs towards the cell cortex converting shrinking MTs to growing ones (*117*). CLIP-170 is composed of two CAP-Gly motifs, which are surrounded by serine-rich regions at its NH_2-terminus, followed by a long coiled-coil structure and two putative metal binding domains at the COOH terminus. It has been demonstrated that CLIP-170 can fold back upon itself through an interaction between its NH_2- and COOH-termini, alternating between an active, extended conformation, in which it can interact with MTs and its COOH-terminal partners, and an inactive, folded conformation, in which it is not bound to other proteins. We recently demonstrated that the loss of CDKL5 negatively impacts the capacity of CLIP-170 to bind to MTs. Considering all the above, we therefore speculated that CLIP-170 is more frequently in its inactive conformation when CDKL5 is lacking explaining its reduced MT binding. For this reason, we decided to analyse whether the conformation of CLIP-170 and, consistently, its functionality might be impaired in CDKL5-deficient cells.

Through *in vivo* FRET analysis on COS7 cells, we found that CLIP-170 is mainly in its closed state in the absence of CDKL5, thus indicating that the kinase could act, directly or indirectly, on its folding (see Results, Fig. 4.1).

CLIP-170 plays a dual role in regulating cell morphology and migration. In normal conditions, MTs are characterized by rapid growth and low catastrophe frequency that allows a persistent growth of MTs. The normal function of CLIPs (including CLIP-170) is to promote MT assembly. Moreover, by modulating the capture of MTs to the cell cortex through the complex formation with IQAGP1, CLIP-170 promotes cell migration (*18*).

Considering that the open conformation of CLIP-170 exposes the two domains involved respectively in modulating MT dynamics and MT capture at the cell cortex, our results might explain the altered phenotypes found in CDKL5-silenced cells. On the one hand, the hypo-functional conformation of CLIP-170, observed in the absence of CDKL5, reduces its binding to MTs, causing their disorganization. On the other hand, in the closed conformation, CLIP-170 is likely to be impaired in its binding to IQGAP1. This could justify, at least in part, the disruption of the Rac1–IQGAP1–CLIP-170 triple complex and the consequent alterations found in CDKL5-deficient cells [Appendix 1, (*14*, *15*, *118*)].

The switching between the open and closed conformations of CLIP-170 has been reported to depend on specific phosphorylation events (*19*). Of note different patterns of CLIP-170 phosphorylation seem to play a fundamental role in enhancing or decreasing the affinity between N- and C-terminal domains regulating the consequent interaction between CLIP-170 and MTs (*119*, *120*). However, the biological significance of differential phosphorylation of CLIP-170 is yet to be addressed. Thus, we cannot exclude that specific events of CLIP-170 phosphorylation may be regulated by CDKL5, which may promote, directly or indirectly, the open conformation of CLIP-170, increasing its capacity to bind to MTs.

5.2 Cdkl5 regulates axonal dynamics via CLIP-170

Because of its involvement in neurological disorders CDKL5 has mostly been studied for its neuronal functions and several reports have described the role of Cdkl5 in regulating neuronal morphology. In line with previous results in *Cdkl5*-silenced neurons (*13*), we confirmed in KO neurons that the loss of Cdkl5 induces a significant reduction of the average axonal length in young neurons and an impaired axon specification. Indeed,

Cdkl5-null neurons were characterized by an increase in the number of neurons bearing either no axon or multiple axons. Interestingly, CLIP-170 was reported to be involved in the modulation of such processes, regulating proper growth cone organization, axon specification and outgrowth by promoting MT stability in axonal growth cones.

During axonal outgrowth, protruding MTs within the growth cone function as a "pushing force" against the actin meshwork allowing the protrusion of the axon (*115*). By moderately enhancing MT stability in the growth cone, +TIPS such as CLIP-170 play an important role in this process (*16*).

Consistent with all the overlapping features between neurons devoid of Cdkl5 and CLIP-170, we found that *Cdkl5*-KO neurons display an altered growth cone morphology characterized by an overall increase in the area occupied by the MTs within the tip of the axon, usually coincident with a paused state (see Results, fig. 4.2). As previously described, growth cones at the tips of rapidly extending axons are small, straight and characterized by highly motile MTs, while in paused axons, MTs become bundled and form loops that cause an enlargement of the structure (*104*). Such morphological alterations on the one hand provide further evidence of a potential role of CDKL5 in the regulation of CLIP-170 activity. Indeed, functional CLIP-170, ensuring a moderate stabilization of MTs (*18*) and allowing their interaction with the actin cytoskeleton, either by physically pushing against the actin network or by inducing actin-related signalling, supports MT polymerization thus allowing their proper dynamics in the axonal growth cone (*121*). On the other hand, the aforementioned growth cone defects may contribute to the other axonal alterations we found in *Cdkl5*-null neurons. Indeed, weakened MT polymerization, caused by reduced binding of CLIP-170, is likely to prevent the ability of MTs to engorge in the area protruded by actin filaments at the tip of the axon. Consequently, the MTs will attain a splayed organization, thus increasing the growth cone size and cause a reduced elongation (see Results, fig. 4.4).

In view of the above we can speculate that CLIP-170 and Cdkl5 may act in common pathways. This prompted us to analyse whether the localization of CLIP-170 in neurons could be affected by the loss of Cdkl5. Firstly, consistent with previous publications, we found that CLIP-170 localizes in the growth cone of axons where it regulates MT dynamics for axon development (*16*). We also demonstrated that the loss of Cdkl5 affects the proper distribution of CLIP-170 in this cellular compartment. Indeed, this

+TIP appeared delocalized from tubulin, reinforcing our data showing a reduced capacity of the protein to bind MTs (see Results, Fig. 4.3). This result, which is supported by the apparently closed conformation of CLIP-170 in CDKL5 depleted COS7 cells, may strengthen our hypothesis that the two proteins act in common pathways. Indeed, Cdkl5 localizes within the axonal growth cone (*8*), where it may regulate, directly or indirectly, the MT binding capacity of CLIP-170.

5.3 Cdkl5, probably acting on CLIP-170, modulates dendritic spine maturation

In the past years Cdkl5 has been linked to the regulation of neurite outgrowth via Rac1 (*8*) and has been found to control proper spine development and stabilization. In fact, the lack of Cdkl5 results in an overall spine loss characterized by an increased number of immature filopodia-like spines and a simultaneous reduction of mature spines (*7*, *9*, *10*, *66*, *75*). These morphological defects have been confirmed in the present study, thanks to the characterization of primary hippocampal neurons derived from *Cdkl5*-KO embryos. Indeed, we found that the loss of Cdkl5 produces a reduction of spine density with a concurrent increase of morphologically immature spines. These data were further supported by the analysis of PSD95 *puncta* that were significantly reduced in *Cdkl5*-KO neurons (see Results, fig. 4.6). PSD95 is an indicator of functionally mature spines and its presence at such level correlates with synaptic strength (*110*). These pieces of evidence, showing a reduced number of PSD95 *puncta* in *Cdkl5*-KO neurons, are further supported by our recent publication in which we demonstrate that the loss of Cdkl5 negatively impacts also on AMPA-receptor membrane exposure, which have been correlated with the formation and maturation of dendritic spines. Thus, altogether these data lend support to the presence of immature spines in *Cdkl5*-null neurons (*12*).
While changes in size and shape of dendritic spines have since long been linked to the remodelling of actin cytoskeleton (*122*), the presence of MTs and the associated proteins has remained a subject of debate till very recently, probably due to their dynamic structure and transient permanence in such compartment. Interestingly, MTs that enter dendritic spines are capable of polymerizing in the correct orientation thanks to the action of the +TIPs that allow the communication between MTs and the actin cytoskeleton (*20*). The +TIP EB3 is required for spine formation and its reduced levels

causes a reduction of their density and morphology (*108*). Moreover, IQGAP1, an interactor of CLIP-170 and other +TIPs, is involved in proper spine formation (*123*, *124*). Thus, even if a direct link between spine formation and CLIP-170 has not been found yet, we speculate that Cdkl5 may control MT dynamics in dendritic spines in a CLIP-170–dependent manner. Bearing in mind that the depletion of CDKL5 causes a reduced functionality of CLIP-170 in COS7 cells, we assume that loss of neuronal Cdkl5 may generate a similar effect, influencing MT dynamics in spines and thereby alter their proper formation and maturation. Our characterization of primary hippocampal neurons gave support to this model. Indeed, using two complementary approaches we could detect CLIP-170 in dendritic spines (see Results, Fig. 4.5), suggesting that it may indeed play a role in the regulation of MT dynamics in such compartment. Furthermore, through a biochemical analysis we found that the loss of Cdkl5 produces a reduction of CLIP-170 levels in the synaptic fraction of mouse brain lysates. This evidence could support our hypothesis that Cdkl5 is fundamental to maintain CLIP-170 in its open conformation in the dendrites, thus promoting MT growth and invasion. On the other side, we cannot exclude that the loss of Cdkl5 may also affect CLIP-170 expression. In fact, CLIP-170 levels were reduced in both the synaptic fraction and in total lysates, suggesting a global decrease of its expression. Further experiments are needed to clarify this point.

Eventually, although PSD95, the levels of which are reduced in *Cdkl5*-KO neurons, is not directly trafficked along MTs into dendritic spines, polymerization of MTs into such compartment is necessary for the synaptic accumulation of PSD95, thus allowing synaptic maturation (*125*). Based on these data, it becomes clear that Cdkl5 may exert a central role in the stabilization of mature spines though its regulation of CLIP-170 and that loss of Cdkl5 disrupts the tight coordination of MT dynamics controlled by CLIP-170 with consequences on downstream events such as synapse stabilization.

5.4 P5 e PME ameliorate Cdkl5-related defects in cells and neurons

CLIP-170 has recently been identified as the cellular receptor for the neurosteroid Pregnenolone. P5, an endogenous steroid generated from cholesterol by the action of CYP11A1, is known to bind and activate CLIP-170 by changing its conformation, thus

potentiating its ability to enhance microtubule assembly and interaction with microtubules and the microtubule-associated proteins (*21*). P5 was demonstrated to be capable of ameliorating CDKL5-related defects both in cycling cells and in neurons: indeed, the treatment with this neurosteroid was able to enhance CLIP-170 binding to MTs in COS7 cells and to correct axonal alterations in primary hippocampal neurons silenced for CDKL5 [Appendix 1, (*14*)].

As an endogenous neurosteroid, P5 can be further metabolized into other steroids that can accomplish different functions: among the metabolites of P5, P5-S and allopregnanolone can target $GABA_A$, NMDA, and Sigma1 receptors and thus modulate neurotransmission (*112*). Conversely, P5 has low affinity for such receptors and its mechanism of action has been reported to involve the above mentioned effect on microtubule dynamics through its direct binding to CLIP-170 and MAP2, another microtubule binding protein (*21*, *111*). Moreover, P5 has lately caught interest by acting as an allosteric negative modulator of the type-1 cannabinoid (CB1) receptor, thus being capable of protecting the brain from cannabis intoxication (*126*). Thus, considering the possible off-target effects of P5 in a future clinical application for CDKL5 disorder, we tested the efficacy of the synthetic compound PME, a non-metabolizable derivative of P5 which promotes MT dynamics (*111*), but is devoid of the effects due to P5 metabolism: indeed in *in vitro* studies this compound did not show affinity for any neurotransmitter receptor of the central nervous system, while demonstrated to enhance tubulin assembly by binding to the microtubule associated protein MAP2 (*22*, *112*, *127*).

Consistent with our previous results, the *in vivo* FRET analysis revealed that both P5 and PME enhance the opened conformation of CLIP-170 in CDKL5 silenced cells (see Results, Fig. 4.7 and 4.8) Our findings confirm previous publication on P5 specific activity on CLIP-170 (*21*) and pave the way for studies on the novel compound PME. Indeed, in accordance with our previous results on P5-treated cells [Appendix 1, (*14*)], PME could restore the association of CLIP-170 with MTs in proliferating CDKL5-deficient cells, apparently bypassing the need of CDKL5. These results could lead to the identification of a novel function of PME on CLIP-170 conformation, which may have interesting implications for patients with mutations in *CDKL5*.

As further support of the relevance of such findings and consistent with our previous results on cycling cells, we found that the neurosteroid Pregnenolone and its synthetic derivative PME are capable of restoring or ameliorating the morphological alterations found in *Cdkl5*-KO neurons. Indeed, both P5 and PME corrected axonal defects reducing the growth cone area and consistently enhancing the percentage of "extending" growth cones. This evidence was further supported by the effect of P5 and PME on the localization of CLIP-170 in growth cones, which overlapped with tubulin suggesting its enhanced interaction with MTs (see Results, fig. 4.9). The action of the compounds on the growth cones may have promoted MTs dynamics in the axonal compartment. Indeed, treatment of young neurons normalized axon specification and outgrowth (see Results, fig. 4.10). Eventually, both neurosteroids ameliorated spine density and morphology in mature *Cdkl5*-KO neurons, increasing the number of PSD95 positive *puncta* and reducing the percentage of immature, thin or filopodia-like, spines (see Results, fig. 4.11).

5.5 Conclusions

Several reports have in the past linked CDKL5 to the regulation of cytoskeletal dynamics [Appendix 1, (*8*, *14*)]. Moreover, very recently, Baltussen and colleagues identified three novel CDKL5 interactors, MAP1S, EB2 and ARHGEF2 (*128*), which, interestingly, are MT associated proteins. All in all, our results disclose a novel role of CDKL5 in the regulation of MT dynamics that depends on its action on CLIP-170. The manifestation of morphological neuronal defects in CDKL5 disorder can well be explained by a deranged MT dynamics caused by dysfunctional CLIP-170 (fig. 5.1). Intriguingly, many neurological diseases are associated with defects in the MT +TIPs genes; among these, the *CLIP-170* gene, also known as *CLIP1*, was linked to autosomal recessive intellectual disability (*109*). This evidence suggests a possible implication of CLIP-170 in the aetiology of the CD, a disorder characterized by intellectual disability.

Moreover, although further studies are needed to fully understand which of the various morphological and molecular CDKL5-associated defects that can possibly be restored by P5 and PME, our studies may have interesting implications for patients with mutations in *CDKL5*. In the brain, reduced levels of P5 have been associated with aging and

neurodegenerative disorders (*129*); it will thus be interesting in the future to analyse whether the levels of P5 or its metabolites are reduced in patients with CDKL5 disorder. If this were the case, considering the neuroprotective potential of P5 (*130*), we can assume that the neuronal damage caused by the frequent seizures in these patients might not be sufficiently attenuated by the neurosteroid. Moreover, administration of P5 was found to enhance memory and cognition in rodents (*131*). In humans, clinical testing of Pregnenolone proved its anti-depressive and anti-psycotic effects and the drug was well tolerated with a positive safety profile (*132*, *133*). The P5 derivative, PME, was synthesized in the early 1950s (*134*) and has since then been tested in several clinical settings. This compound was firstly experimented for the treatment of arthritis and hypersensitivity disease. Although PME did not show any apparent toxic properties and no androgenic or estrogenic effects were observed in extensive tests on rats, no actual decrease was seen either in the arthritic process in patients receiving this compound. Intriguingly however, the treatment produced a feeling of well-being in patients, who displayed reduced anxiety. PME was therefore suggested as a promising compound for psychiatric diseases. The first clinical trial on psychiatric symptoms was carried out on 150 patients. No significant changes were noted in disorders affecting content of thought, but the compound demonstrated to be effective in decreasing irritability, anxiety and depression (*135*). More recently, two studies conducted on rodents demonstrated that PME could be a useful treatment for depressive disorders (*22*, *136*). Indeed, the development of synthetic steroids maintaining the specific action of P5 may lead to the development of interesting therapeutic compounds for various neurological disorders, including CD.

Therapeutic strategies, including drug-based therapies, are still missing for patients with CDKL5 disorder. Based on our results, we find it intriguing to speculate that P5 and PME, targeting CLIP-170, might represent interesting candidates for this group of patients. To test further the therapeutic potential of both compounds for CD, *in vivo* studies will be performed, in which behavioural tests will be conducted on treated *Cdkl5*-KO mice.

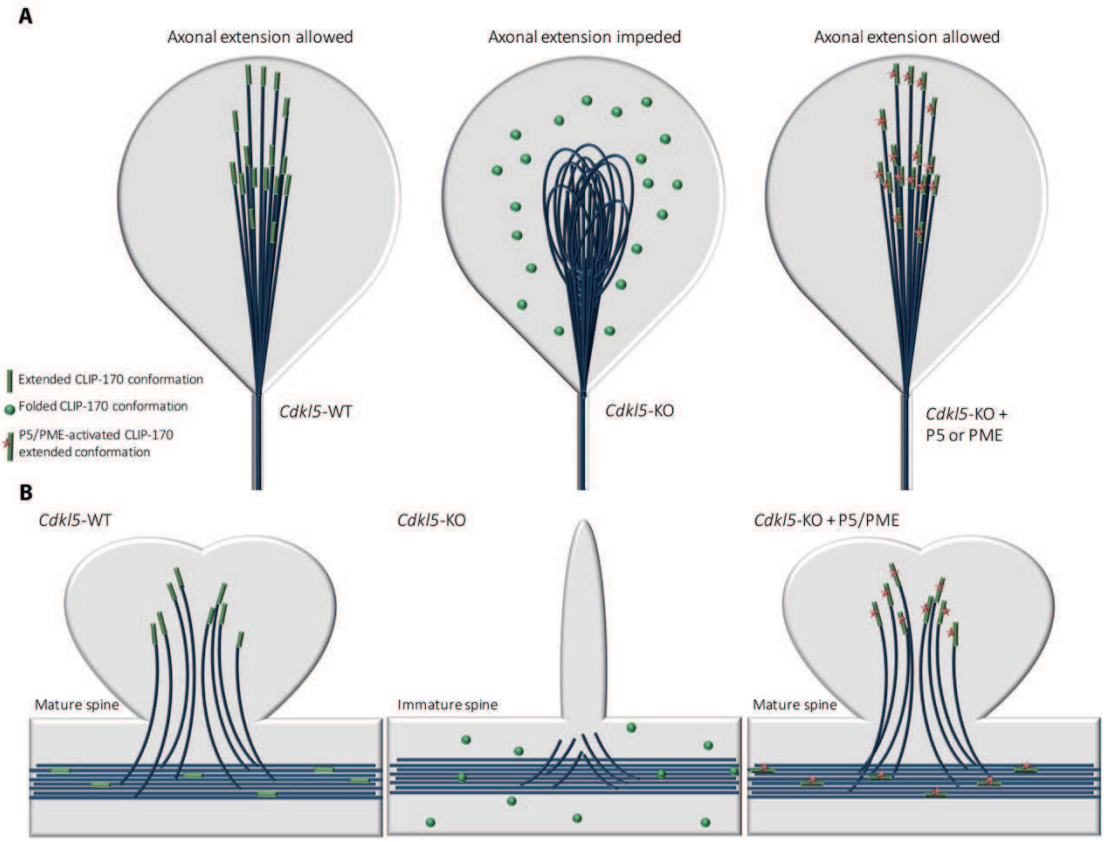

Fig. 5.1 Proposed model: CDKL5 alters CLIP-170 conformation and activity in axonal growth cones and spines. (A) In *Cdkl5*-WT axons, CLIP-170, in its active extended conformation, binds to MTs, which are properly organized, can polymerize and allow axon specification, elongation, and proper growth cone morphology. In *Cdkl5*-KO axons CLIP-170, in its inactive folded conformation, cannot interact with MTs, which appear disorganized and unable to polymerize, impairing proper axonal development. The treatment with P5 or PME is able to stabilize CLIP-170 active conformation, allowing MT polymerization and dynamics, favouring axonal extension. (B) In *Cdkl5*-WT dendrites, CLIP-170, in its extended conformation, binds to MTs, which can polymerize and are driven into spines, allowing their formation and maturation. In *Cdkl5*-KO dendrites, CLIP-170, in its folded conformation, cannot interact with MTs, which appear unable to polymerize and to protrude within the spine, thus impairing proper spine development. The treatment with P5 or PME is able to stabilize CLIP-170 active conformation, allowing MT polymerization and dynamics, promoting spine formation and maturation.

Bibliography

1. V. M. Kalscheuer *et al.*, Disruption of the Serine / Threonine Kinase 9 Gene Causes Severe X-Linked Infantile Spasms and Mental Retardation. *Am. J. Hum. Genet.* **72**, 1401–1411 (2003).
2. S. Fehr *et al.*, The CDKL5 disorder is an independent clinical entity associated with early-onset encephalopathy. *Eur. J. Hum. Genet.* **21**, 266–73 (2013).
3. E. Montini *et al.*, Identification and Characterization of a Novel Serine– Threonine Kinase Gene from the Xp22 Region. *Genomics.* **433**, 427–433 (1998).
4. F. Mari *et al.*, CDKL5 belongs to the same molecular pathway of MeCP2 and it is responsible for the early-onset seizure variant of Rett syndrome. *Hum. Mol. Genet.* **14**, 1935–1946 (2005).
5. I. Kameshita *et al.*, Cyclin-dependent kinase-like 5 binds and phosphorylates DNA methyltransferase 1. *Biochem. Biophys. Res. Commun.* **377**, 1162–1167 (2008).
6. S. Ricciardi, C. Kilstrup-nielsen, T. Bienvenu, V. Broccoli, CDKL5 influences RNA splicing activity by its association to the nuclear speckle molecular machinery. *Hum. Mol. Genet.* **18**, 4590–4602 (2009).
7. S. Trazzi *et al.*, HDAC4: A Key Factor Underlying Brain Developmental Alterations in CDKL5 Disorder. *Hum. Mol. Genet.* **0**, 1–21 (2016).
8. Q. Chen *et al.*, CDKL5, a Protein Associated with Rett Syndrome, Regulates Neuronal Morphogenesis via Rac1 Signaling. *J. Neurosci.* **30**, 12777–12786 (2010).
9. S. Ricciardi *et al.*, CDKL5 ensures excitatory synapse stability by reinforcing NGL-1-PSD95 interaction in the postsynaptic compartment and is impaired in patient iPSC-derived neurons. *Nat. Cell Biol.* **14**, 911–23 (2012).
10. Y. Zhu *et al.*, Palmitoylation-dependent CDKL5–PSD-95 interaction regulates synaptic targeting of CDKL5 and dendritic spine development. *Proc. Natl. Acad. Sci.* **110**, 9118–9123 (2013).
11. M. Sekiguchi *et al.*, Identification of amphiphysin 1 as an endogenous substrate for CDKL5 , a protein kinase associated with X-linked neurodevelopmental disorder. *Biochem. Biophys. Res. Commun.* **535**, 257–267 (2013).
12. M. Tramarin *et al.*, The antidepressant tianeptine reverts synaptic AMPA receptor defects caused by deficiency of CDKL5. *Hum. Mol. Genet.* **4** (2018).
13. M. S. Nawaz *et al.*, CDKL5 and shootin1 interact and concur in regulating neuronal polarization. *PLoS One*. **11** (2016).
14. I. Barbiero *et al.*, The neurosteroid pregnenolone reverts microtubule derangement induced by the loss of a functional CDKL5-IQGAP1 complex. **26**, 3520–3530 (2017).
15. M. Fukata *et al.*, Rac1 and Cdc42 capture microtubules through IQGAP1 and CLIP-170. *Cell*. **109**, 873–885 (2002).
16. D. Neukirchen, F. Bradke, Cytoplasmic Linker Proteins Regulate Neuronal Polarization through Microtubule and Growth Cone Dynamics. *J. Neurosci.* **31**, 1528–1538 (2011).

17. L. Swiech *et al.*, CLIP-170 and IQGAP1 cooperatively regulate dendrite morphology. *J. Neurosci.* **31**, 4555–68 (2011).

18. Y. A. Komarova, A. S. Akhmanova, S. I. Kojima, N. Galjart, G. G. Borisy, Cytoplasmic linker proteins promote microtubule rescue in vivo. *J. Cell Biol.* **159**, 589–599 (2002).

19. G. Lansbergen *et al.*, Conformational changes in CLIP-170 regulate its binding to microtubules and dynactin localization. *J. Cell Biol.* **166**, 1003–1014 (2004).

20. E. W. Dent, W. Bement, Of microtubules and memory: implications for microtubule dynamics in dendrites and spines. *Mol. Biol. Cell*. **28**, 1–8 (2017).

21. C.-H. Weng *et al.*, Pregnenolone activates CLIP-170 to promote microtubule growth and cell migration. *Nat. Cell Biol.* **9**, 636–42 (2013).

22. M. Bianchi, E. Baulieu, 3β-Methoxy-pregnenolone (MAP4343) as an innovative therapeutic approach for depressive disorders. *Proc. Natl. Acad. Sci. U. S. A.* **109**, 1713–1718 (2012).

23. B. Hagberg, P. Rasmussen, "Forme fruste of Rett Syndrome - A case report. *Acta Paediatr. Scand. Suppl.* **181**, 175–181 (1986).

24. A. Rett, On a unusual brain atrophy syndrome in hyperammonemia in childhood. *Wien. Med. Wochenschr.* **116**, 723–6 (1966).

25. B. Hagberg, Clinical manifestations and stages of Rett Syndrome. *Ment. Retard. Dev. Disabil. Res. Rev.* **8**, 61–65 (2002).

26. Y. Nomura, Early behavior characteristics and sleep disturbance in Rett syndrome. *Brain Dev.* **27** (2005).

27. M. Chahrour, H. Y. Zoghbi, Review The Story of Rett Syndrome: From Clinic to Neurobiology. *Neuron*. **56**, 422–437 (2007).

28. S. J. Williamson, J. Christodoulou, Rett syndrome: new clinical and molecular insights. *Eur. J. Hum. Genet.* **14**, 896–903 (2006).

29. B. A. Hagberg, O. H. Skjeldal, Rett Variants: A Suggested Model for Inclusion Criteria. *Pediatr. Neurol.* **11**, 5–11 (1994).

30. A. K. Percy *et al.*, Rett Syndrome: North American Database. *J. Child Neurol.* **22**, 1338–1341 (1928).

31. F. Hanefeld, The clinical pattern of the rett syndrome. *Brain Dev.* **7**, 320–325 (1985).

32. J. C. Evans *et al.*, Early onset seizures and Rett-like features associated with mutations in CDKL5. *Eur. J. Hum. Genet.* **13**, 1113–20 (2005).

33. L. Huopaniemi, H. Tyynismaa, A. Rantala, T. Rosenberg, Characterization of Two Unusual RS1 Gene Deletions Segregating in Danish Retinoschisis Families. *Hum. Mutat.* **16**, 307–314 (2000).

34. J. Tao *et al.*, Report Mutations in the X-Linked Cyclin-Dependent Kinase – Like 5 (CDKL5 / STK9) Gene Are Associated with Severe Neurodevelopmental Retardation. *Am. J. Hum. Genet.* **75**, 1149–1154 (2004).

35. L. S. Weaving *et al.*, Mutations of CDKL5 Cause a Severe Neurodevelopmental Disorder with Infantile Spasms and Mental Retardation. *Am. J. Hum. Genet.* **74**, 1079–1093 (2004).

36. E. Scala *et al.*, CDKL5/STK9 is mutated in Rett syndrome variant with infantile spasms. *J Med Genet* **42**, 103–107 (2005).

37. N. Bahi-Buisson *et al.*, Key clinical features to identify girls with CDKL5 mutations. *Brain*. **131**, 2647–2661 (2008).

38. N. Bahi-Buisson *et al.*, The three stages of epilepsy in patients with CDKL5 mutations. *Epilepsia*. **49**, 1027–1037 (2008).

39. R. Artuso *et al.*, Early-onset seizure variant of Rett syndrome: Definition of the clinical diagnostic criteria. *Brain Dev* **32**, 17–24 (2010).

40. L. Neul *et al.*, Rett Syndrome: Revised Diagnostic Criteria and Nomenclature. *Ann Neurol*. **68**, 944–950 (2010).

41. C. Kilstrup-Nielsen *et al.*, What we know and would like to know about CDKL5 and its involvement in epileptic encephalopathy. *Neural Plast* **2012**, 1–11 (2012).

42. S. L. Williamson *et al.*, A novel transcript of cyclin-dependent kinase-like 5 (CDKL5) has an alternative C-terminus and is the predominant transcript in brain. *Hum Genet* **5**, 187–200 (2012).

43. R. D. Hector *et al.*, Characterisation of CDKL5 Transcript Isoforms in Human and Mouse. *PLoS One*. **11**, 1–22 (2016).

44. I. Bertani *et al.*, Functional Consequences of Mutations in Functional Consequences of Mutations in CDKL5 , an X-linked Gene Involved in Infantile Spasms and Mental Retardation. *J Biol Chem* **281**, 32048–32056 (2006).

45. G. Pearson *et al.*, Mitogen-Activated Protein (MAP) Kinase Pathways: Regulation and Physiological Functions. *Endocr Rev* **22**, 153–183 (2001).

46. S. Katayama, N. Sueyoshi, I. Kameshita, Critical Determinants of Substrate Recognition by Cyclin-Dependent Kinase-like 5 (CDKL5). *Biochem Biophys Res Commun*. **54**, 2975–2987 (2015).

47. D. L. Bodian, M. Schreiber, T. Vilboux, A. Khromykh, N. S. Hauser, Mutation in an alternative transcript of CDKL5 in a boy with early-onset seizures. *Cold Spring Harb Mol Case Stud* **4**, 1–10 (2018).

48. R. D. Hector *et al.*, CDKL5 variants Improving our understanding of a rare neurologic disorder. **0**, 1–10 (2017).

49. L. Rusconi *et al.*, CDKL5 expression is modulated during neuronal development and its subcellular distribution is tightly regulated by the C-terminal tail. *J Biol Chem* **283**, 30101–30111 (2008).

50. S. Fehr *et al.*, Seizure variables and their relationship to genotype and functional abilities in the CDKL5 disorder. *Neurology*. **87**, 1–8 (2016).

51. P. Szafranski *et al.*, Neurodevelopmental and neurobehavioral characteristics in males and females with CDKL5 duplications. *Eur J Hum Genet* **23**, 915–921 (2015).

52. A. Zhou, S. Han, G. Li, Zhou, Molecular and genetic insights into an infantile epileptic encephalopathy – CDKL5 disorder. *Front Biol*. **12**, 1–6 (2017).

53. S. Fehr *et al.*, Functional Abilities in Children and Adults with the CDKL5 Disorder. *J Med Genet*

enet **5**, 2860–2869 (2016).

54. R. oncu, A. Efeyan, D. M. Sabatini, mTOR: from growth signal integration to cancer, diabetes and ageing. *at Pu l* **12**, 21–35 (2010).

55. I. Wang *et al.*, Loss of CDKL5 disrupts kinome profile and event-related potentials leading to autistic-like phenotypes in mice. *P* . **109**, 21516–21521 (2012).

56. E. Amendola *et al.*, Mapping Pathological Phenotypes in a Mouse Model of CDKL5 Disorder. *PLo ne*. **9**, 5–16 (2014).

57. S. Ricciardi *et al.*, Reduced AKT / mTOR signaling and protein synthesis dysregulation in a Rett syndrome animal model. *u Mol enet* **20**, 1182–1196 (2011).

58. Chen, I. Alberts, X. Li, Dysregulation of the IGF-I / PI3K / AKT / mTOR signaling pathway in autism spectrum disorders. *nt Dev eu b c* **35**, 35–41 (2014).

59. C. Fuchs *et al.*, Loss of CDKL5 impairs survival and dendritic growth of newborn neurons by altering AKT / GSK-3 signaling. *eu b bl D* **70**, 53–68 (2014).

60. Luo, The role of GSK3beta in the development of the central nervous system. *ont bl*. **7**, 212–220 (2012).

61. I. Barbiero *et al.*, CDKL5 localizes at the centrosome and midbody and is required for faithful cell division. *c ep* **7**, 1–12 (2017).

62. C. Ernst, Proliferation and Differentiation De fi cits are a Major Convergence Point for Neurodevelopmental Disorders. *end eu b c* **39**, 290–299 (2016).

63. H. Li, X. hong, K. F. Chau, E. C. Williams, Q. Chang, Loss of activity-induced phosphorylation of MeCP2 enhances synaptogenesis , LTP and spatial memory. *at Pu l* **14**, 1001–1008 (2011).

64. S. Cohen *et al.*, Genome-Wide Activity-Dependent MeCP2 Phosphorylation Regulates Nervous System Development and Function. *eu bn*. **72**, 72–85 (2011).

65. A. Bergo *et al.*, Methyl-CpG Binding Protein 2 (MeCP2) Localizes at the Centrosome and Is Required for Proper Mitotic Spindle. *bl C e* **290**, 3223–3237 (2015).

66. G. Della Sala *et al.*, Dendritic Spine Instability in a Mouse Model of CDKL5 Disorder Is Rescued by Insulin-like Growth Factor 1. *bl P c at* . **80**, 1–10 (2015).

67. M. Toriyama *et al.*, Shootin1: a protein involved in the organization of an asymmetric signal for neuronal polarization. *Cell bl* **175**, 147–157 (2006).

68. G. A. Ramakers, Rho proteins, mental retardation and the cellular basis of cognition. *end eu b c* **24**, 191–199 (2002).

69. A. C. Hedman, M. Smith, D. B. Sacks, The biology of IQGAP proteins: beyond the cytoskeleton. *EM ep*. **16**, 427–446 (2015).

70. H. L. Archer *et al.*, CDKL5 mutations cause infantile spasms, early onset seizures, and severe mental retardation in female patients. *Med enet* **43**, 729–734 (2006).

71. C. hang, T. Huang, Y. Hsueh, W. Liao, Mice lacking cyclin-dependent kinase-like 5 manifest autistic and ADHD-like behaviors. *u Mol enet* **26**, 3922–3934 (2017).

72. X. S. Tang *et al.*, Loss of CDKL5 in Glutamatergic Neurons Disrupts Hippocampal Microcircuitry

and Leads to Memory Impairment in Mice. *eu* **37**, 7420–7437 (2017).

73. K. Okuda *et al*, CDKL5 controls postsynaptic localization of GluN2B-containing NMDA receptors in the hippocampus and regulates seizure susceptibility. *eu* **106**, 158–170 (2017).

74. C. Fuchs *et al*, Heterozygous CDKL5 Knockout Female Mice Are a Valuable Animal Model for CDKL5 Disorder. *eu al Pla* **2018**, 1–18 (2018).

75. C. Fuchs *et al*, Inhibition of GSK3 rescues hippocampal development and learning in a mouse model of CDKL5 disorder. *eu* **82**, 298–310 (2015).

76. C. Fuchs *et al*, Treatment with the GSK3-beta inhibitor Tideglusib improves hippocampal development and memory performance in juvenile , but not adult , Cdkl5 knockout mice. *Eu* *eu* **47**, 1054–1066 (2018).

77. L. Pozzo-Miller, S. Pati, A. K. Percy, A. K. Percy, Rett Syndrome Reaching for Clinical Trials. *eu* **12**, 631–640 (2015).

78. M. Kuijpers, C. C. Hoogenraad, Molecular and Cellular Neuroscience Centrosomes , microtubules and neuronal development. *Mol Cell* *eu* **48**, 349–358 (2011).

79. C. C. Hoogenraad, F. Bradke, Control of neuronal polarity and plasticity – a renaissance for microtubules, 669–676 (2009).

80. C. anke, M. Kneussel, Tubulin post-translational modifications: Encoding functions on the neuronal microtubule cytoskeleton. *end* *eu* **33**, 362–372 (2010).

81. R. Subramanian, T. M. Kapoor, Building Complexity: Insights into Self-organized Assembly of Microtubule-based Architectures. *Dev Cell*. **23**, 874–885 (2012).

82. S. Maday, A. E. Twelvetrees, A. Moughamian, E. L. F. Holzbaur, Review Axonal Transport Cargo-Specific Mechanisms of Motility and Regulation. *eu on*. **84**, 292–309 (2014).

83. R. Rivas, M. E. Hatten, Motility and Cytoskeletal Granule Neurons Organization of Migrating Cerebellar. *eu* **5**, 981–989 (1995).

84. E. W. Dent, S. L. Gupton, F. B. Gertler, The Growth Cone Cytoskeleton in Axon outgrowth and guidance. *Cold pn a Pe pect* **3**, 1–40 (2011).

85. D. M. Suter, K. E. Miller, The Emerging Role of Forces in Axonal Elongation Daniel. *P* *eu* **94**, 91–101 (2011).

86. aworski *et al*, Dynamic Microtubules Regulate Dendritic Spine Morphology and Synaptic Plasticity. *eu on*. **61**, 85–100 (2009).

87. L. C. Kapitein, C. C. Hoogenraad, Review Building the Neuronal Microtubule Cytoskeleton. *eu on*. **87**, 492–506 (2015).

88. Lipka, M. Kuijpers, aworski, C. C. Hoogenraad, Mutations in cytoplasmic dynein and its regulators cause malformations of cortical development and neurodegenerative diseases. *bc e oc an* **4**, 1605–1612 (2013).

89. O. Reiner, T. Sapir, LIS1 functions in normal development and disease. *Cu p eu* **23**, 951–956 (2013).

90. S. Millecamps, ulien, Axonal transport deficits and neurodegenerative diseases. *at ev*

eu b c **14**, 161–176 (2013).

91. C. D. Sorbara *et al.*, Pervasive Axonal Transport Deficits in Multiple Sclerosis Models. *eu on*. **84**, 1183–1190 (2014).

92. K. R. Brunden *et al.*, Epothilone D Improves Microtubule Density, Axonal Integrity and Cognition in a Transgenic Mouse Model of Tauopathy. *eu o c* **30**, 13861–13866 (2011).

93. S. Oz *et al.*, The NAP motif of activity-dependent neuroprotective protein (ADNP) regulates dendritic spines through microtubule end binding proteins. *Mol P*, 1–10 (2014).

94. S. Oz, Y. Ivashko-pachima, I. Gozes, The ADNP Derived Peptide , NAP Modulates the Tubulin Pool Implication for Neurotrophic and Neuroprotective Activities. *PLo ne*. **7**, 1–13 (2012).

95. S. Quraishe, C. M. Cowan, A. Mudher, NAP (davunetide) rescues neuronal dysfunction in a Drosophila model of tauopathy. *Mol P c rt*. **18**, 834–842 (2013).

96. H. Y. Meltzer, S. R. McGurk, The Effects of Clozapine , Risperidone , and Olanzapine on Cognitive Function in Schizophrenia. *c o ull* **25**, 233–256 (1999).

97. L. C. Politte, C. A. Henry, C. Mcdougle, Psychopharmacological Interventions in Autism Spectrum Disorder. *a va d ev p c rt*. **22**, 76–92 (2014).

98. A. Altun, Melatonin therapeutic and clinical utilization. *nt Cl n P act* **61**, 835–845 (2007).

99. B. Prieto-gmez *et al.*, Melatonin attenuates the decrement of dendritic protein MAP-2 immuno-staining in the hippocampal CA1 and CA3 fields of the aging male rat. *eu o c Lett* **448**, 56–61 (2008).

100. F. Marchisella, E. T. Coffey, P. Hollos, Microtubule and Microtubule Associated Protein Anomalies in Psychiatric Disease. *C to keleton*. **0**, 1–16 (2016).

101. L. Parsys *et al.*, Effects of the Synthetic Neurosteroid 3 - Methoxypregnenolone (MAP4343) on Behavioral and Physiological Alterations Provoked by Chronic Psychosocial Stress in Tree Shrews. *nt eu op c op a acol* **19**, 1–12 (2016).

102. K. Murakami, A. Fellous, E. Baulieu, P. Robel, Pregnenolone binds to microtubule-associated protein 2 and stimulates microtubule assembly. *P*. **97**, 3579–3584 (2000).

103. R. G. Goold, R. Owen, P. R. Gordon-weeks, Glycogen synthase kinase 3 phosphorylation of microtubule-associated protein 1B regulates the stability of microtubules in growth cones. *Cell c* **112**, 3373–3384 (1999).

104. E. W. Dent, K. Kalil, Axon Branching Requires Interactions between Dynamic Microtubules and Actin Filaments. *eu o c* **21**, 9757–9769 (2001).

105. S. Geraldo, P. R. Gordon-Weeks, Cytoskeletal dynamics in growth-cone steering. *Cell c* **122**, 3595–3604 (2009).

106. Y. Ren, D. M. Suter, Increase in Growth Cone Size Correlates with Decrease in Neurite Growth Rate. *eu al Pla t* **2016**, 20–22 (2016).

107. T. Tada, M. Sheng, Molecular mechanisms of dendritic spine morphogenesis. *Cu p h eu b bl* **16**, 95–101 (2006).

108. Gu, B. L. Firestein, Q. heng, Microtubules in dendritic spine development. *eu o c* **28**,

12120–12124 (2008).

109. F. Larti *et al.*, A defect in the CLIP1 gene (CLIP-170) can cause autosomal recessive intellectual disability. *Eu* *u* *enet* **23**, 331–336 (2015).

110. A. E. El-Husseini, E. Schnell, D. M. Chetkovich, R. A. Nicoll, D. S. Bredt, PSD-95 Involvement in Maturation of Excitatory Synapses. *cence* *80* **290**, 1364–1369 (2000).

111. V. Fontaine-Lenoir, Y. Duchossoy, E. Baulieu, P. Robel, Microtubule-associated protein 2 (MAP2) is a neurosteroid receptor. *P* . **103**, 4711–4716 (2006).

112. Weng, B. Chung, Nongenomic actions of neurosteroid pregnenolone and its metabolites. *te* *o* *l* **111**, 54–59 (2016).

113. H.- Hsu, M.-R. Liang, C.-T. Chen, B. Chung, Pregnenolone stabilizes microtubules and promotes zebrafish embryonic cell movement. *atu* *e*. **439**, 480–483 (2006).

114. K. A. Dragestein *et al.*, Dynamic behavior of GFP – CLIP-170 reveals fast protein turnover on microtubule plus ends. *Cell* *l* **180**, 729–737 (2008).

115. H. Witte, F. Bradke, The role of the cytoskeleton during neuronal polarization. *Cu* *p* *eu* *o* *l* **18**, 479–487 (2008).

116. P. La Montanara *et al.*, Synaptic synthesis, dephosphorylation, and degradation: A novel paradigm for an activity-dependent neuronal control of CDKL5. *l* *Ce* **290**, 4512–4527 (2015).

117. N. Galjart, Clips and Clasps and cellular dynamics. *at* *ev* *Mol* *Cell* *l* **6**, 487–498 (2005).

118. T. Watanabe *et al.*, Interaction with IQGAP1 links APC to Rac1, Cdc42, and actin filaments during cell polarization and migration. *Dev* *Cell*. **7**, 871–883 (2004).

119. X. Yang *et al.*, Cdc2-mediated Phosphorylation of CLIP-170 Is Essential for Its Inhibition of Centrosome Reduplication. *l* *Ce* **284**, 28775–28782 (2009).

120. H. Choi *et al.*, The FKBP12-rapamycin-associated protein (FRAP) is a CLIP-170 kinase. *EM* *ep*. **3**, 988–994 (2002).

121. H. Witte, D. Neukirchen, F. Bradke, Microtubule stabilization specifies initial neuronal polarization. *Cell* *l* **180**, 619–632 (2008).

122. B. Calabrese, S. Margaret, S. Halpain, Development and Regulation of Dendritic Spine Synapses. *P* *lo* . **21**, 38–47 (2018).

123. I. ausoro *et al.*, Regulation of Spine Density and Morphology by IQGAP1 Protein Domains. *PLo* *ne*. **8**, 1–10 (2013).

124. C. Gao, S. F. Frausto, A. L. Guedea, N. C. Tronson, V. ovasevic, IQGAP1 regulates NR2A signaling, spine density, and cognitive processes. *eu* *o* *c* **31**, 8533–8542 (2011).

125. X. Hu *et al.*, BDNF-induced Increase of PSD-95 in Dendritic Spines Requires Dynamic Microtubule Invasions. *eu* *o* *c* **31**, 15597–15603 (2011).

126. M. Vall e *et al.*, Pregnenolone Can Protect the Brain from Cannabis Intoxication Monique. *cence* *80* **343**, 94–98 (2014).

127. Y. Duchossoy, S. David, E. Emile, P. Robel, Treatment of experimental spinal cord injury with 3 - methoxy-pregnenolone. *b* *e* **1403**, 57–66 (2011).

128. L. L. Baltussen *et al.*, Chemical genetic identification of CDKL 5 substrates reveals its role in neuronal microtubule dynamics. *EM* **2018**, 1–18 (2018).

129. S. Luchetti *et al.*, Neurosteroid biosynthetic pathways changes in prefrontal cortex in Alzheimer ' s disease. . **32**, 1964–1976 (2011).

130. K. Wojtal, M. K. Trojnar, S. Czuczwar, Endogenous neuroprotective factors neurosteroids. *Pa acol epo t.* **58**, 335–340 (2016).

131. F. Flood, E. Morley, E. Robertst, Memory-enhancing effects in male mice of pregnenolone. *eu b blo.* **89**, 1567–1571 (1992).

132. E. S. Brown *et al.*, A Randomized , Double-Blind , Placebo-Controlled Trial of Pregnenolone for Bipolar Depression. *eu bp c op a acolo.* **39**, 2867–2873 (2014).

133. I. Osuji, E. Vera-bolaos, T. Carmody, E. S. Brown, Pregnenolone for cognition and mood in dual diagnosis patients. *P c at e* **178**, 309–312 (2010).

134. M. N. Huffman, W. Sadler, The preparation of 3-methoxy--steroids. *kla o a Med e h t*, 919–927 (1953).

135. G. Harold, M. Sleeper, Experimental use of PME in treating psychiatric symptoms. *D e v t*, 93–94 (1955).

136. Prenderville, M. Bianchi, G. Di Capua, C. McDonnell, Rouine, Single administration of ketamine and Pregnenolone-Methyl-Ether (3-Methoxy-Pregnenolone) has antidepressant efficacy in a preclinical model of treatment resistant depression: identification of a plasma biomarker of pharmacological efficacy. *ht eu bp c op a acol* **40**, 1 (2016).